Soft and Hard X-Ray Microscopy

David Attwood
University of California, Berkeley

and

Advanced Light Source, LBNL

Cheiron School
October 2010
SPring-8

The short wavelength region of the electromagnetic spectrum

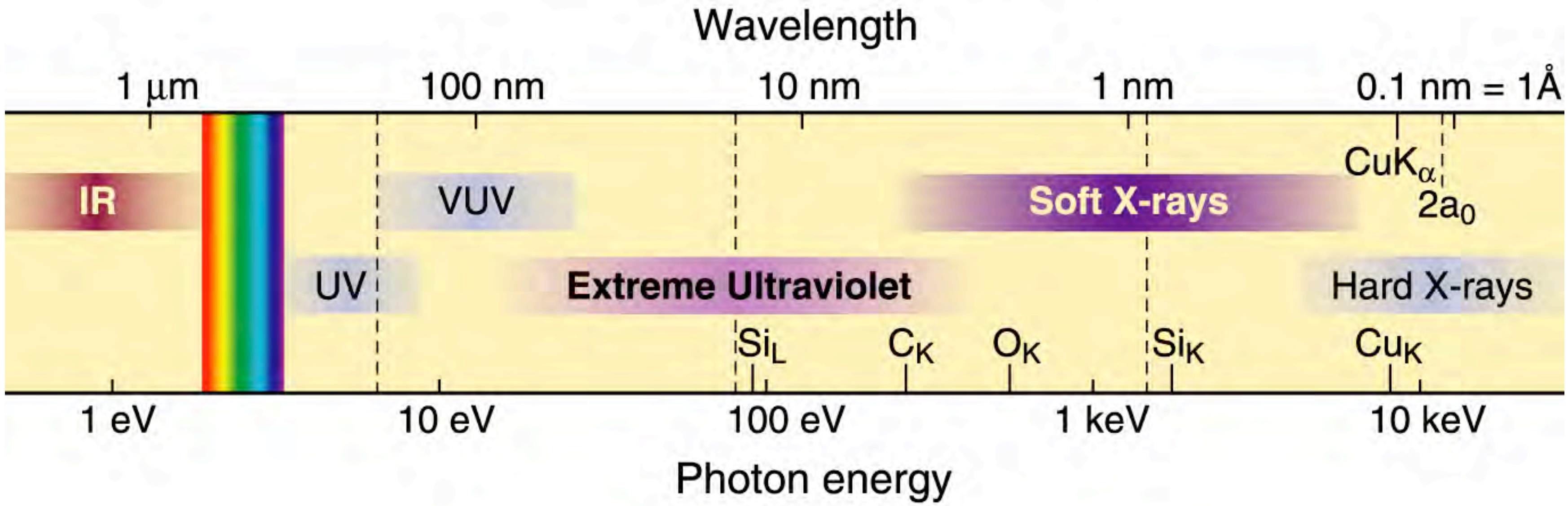

- See smaller features
- Write smaller patterns
- Elemental and chemical sensitivity

$$\hbar\omega \cdot \lambda = hc = 1239.842 \text{ eV nm}$$

$$n = 1 - \delta + i\beta \qquad \delta, \beta << 1$$

Two common soft x-ray microscopes

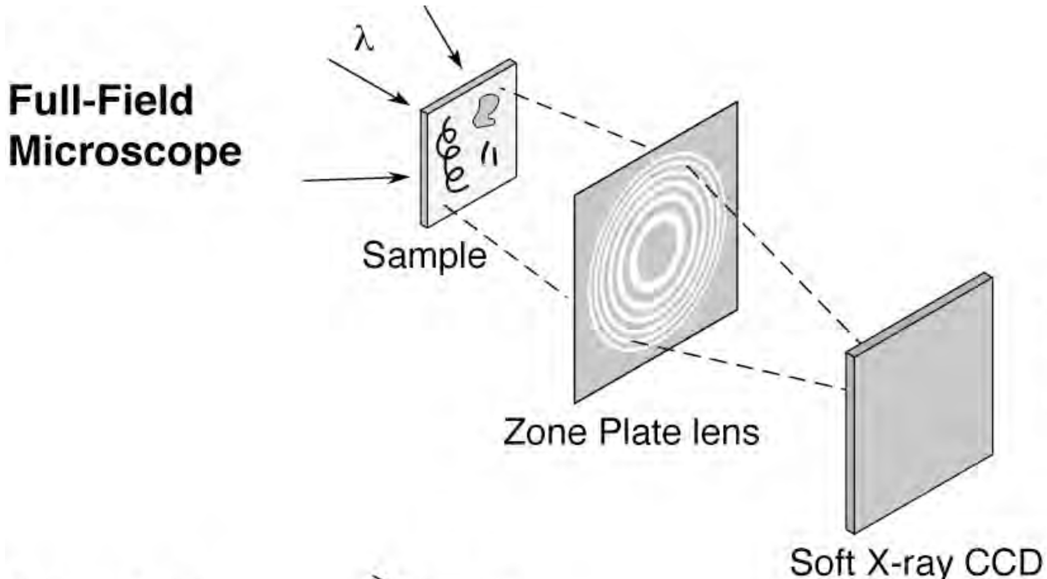

- 10–20 nm spatial resolution
- Modest spectral resolution
- Seconds exposure time
- Bending magnet radiation
- Higher radiation dose
- Flexible sample environment (wet, cryo, labeled magnetic fields, electric fields, cement, ...)

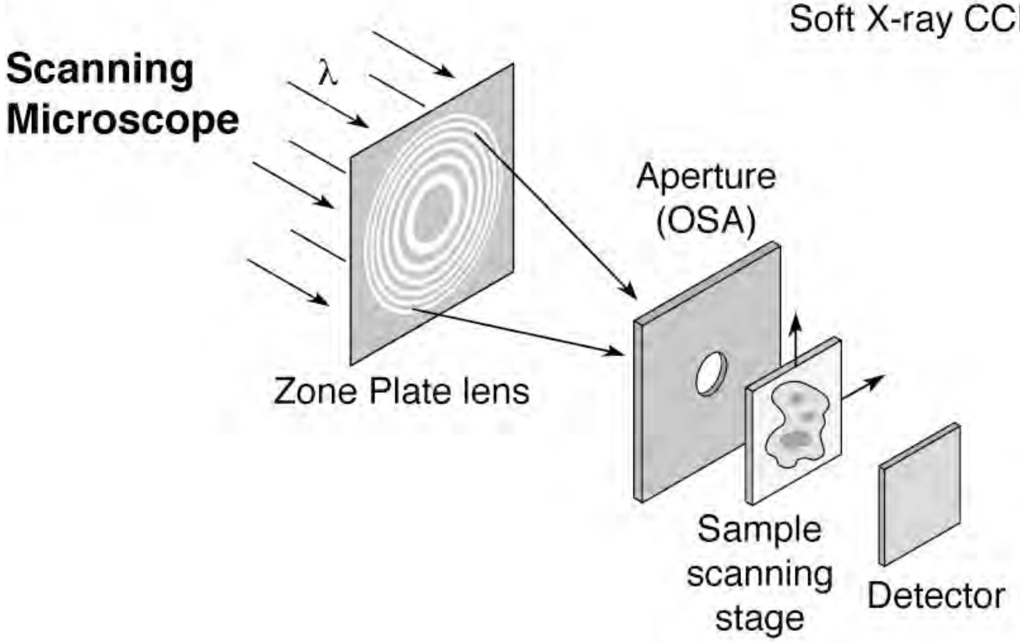

- 10–20 nm spatial resolution
- Least radiation dose
- Best spectral resolution
- Requires spatially coherent radiation
- Minutes exposure time
- Flexible sample environment
- Photoemission, fluorescence imaging

Ch09_F21_Sept2010.ai

A Fresnel zone plate lens for x-ray microscopy

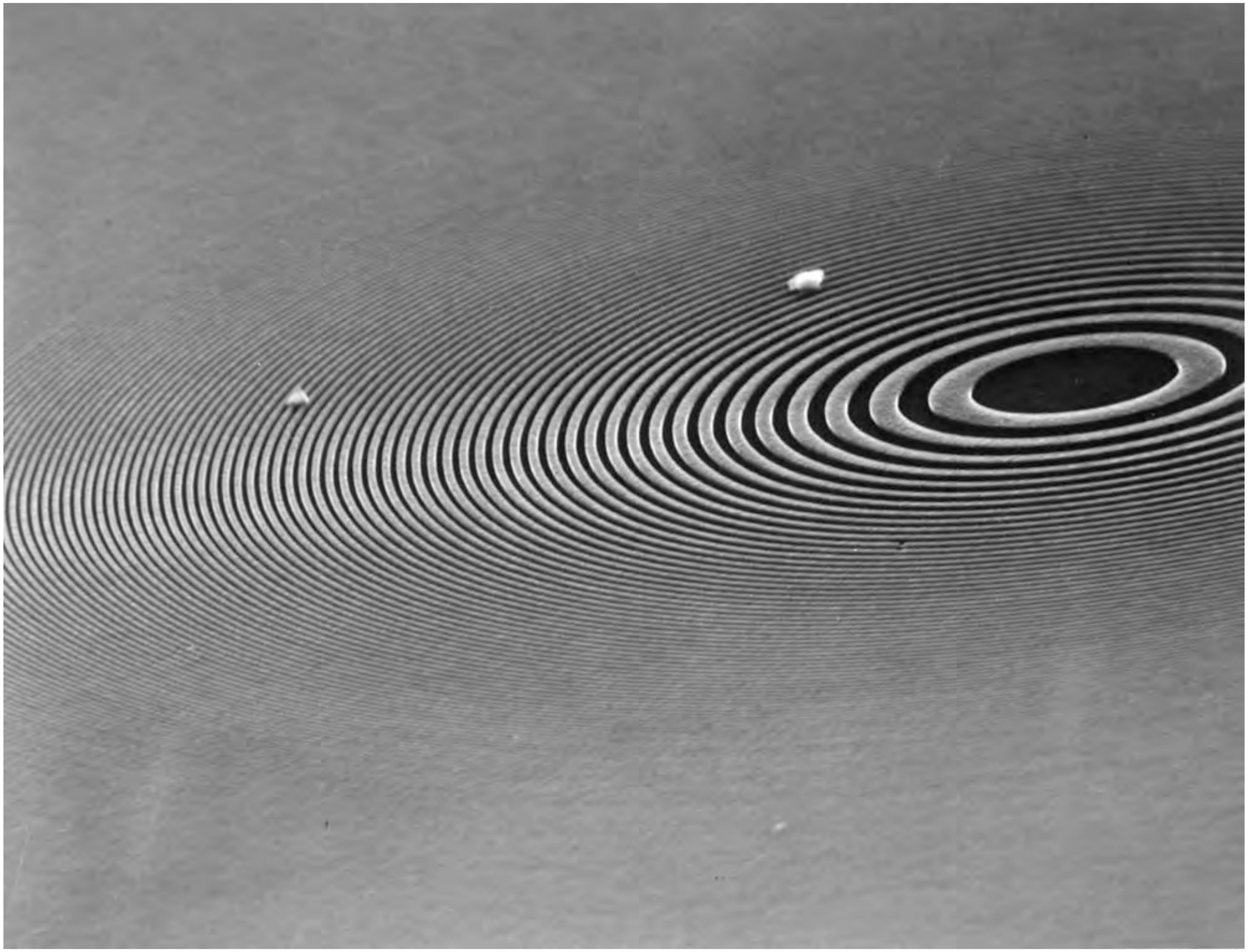

Erik Anderson, LBNL

Nature

LETTERS

Vol 435|30 June 2005|doi:10.1038/nature-3719

Soft X-ray microscopy at a spatial resolution better than 15 nm

Weilun Chao[1,2], Bruce D. Harteneck[1], J. Alexander Liddle[1], Erik H. Anderson[1] & David T. Attwood[1,2]

λ = 1.52 nm (815 eV)
Δr = 15 nm
N = 500
D = 30 µm
f = 300 µm
σ = 0.38
0.8 Δr = 12 nm

Analytical tools that have spatial resolution at the nanometre scale are indispensable for the life and physical sciences. It is desirable that these tools also permit elemental and chemical identification on a scale of 10 nm or less, with large penetration depths. A variety of techniques[1–7] in X-ray imaging are currently being developed that may provide these combined capabilities. Here we report the achievement of sub-15-nm spatial resolution with a soft X-ray microscope—and a clear path to below 10 nm—using an overlay technique for zone plate fabrication. The microscope covers a spectral range from a photon energy of 250 eV (~5 nm wavelength) to 1.8 keV (~0.7 nm), so that primary K and L atomic resonances of elements such as C, N, O, Al, Ti, Fe, Co and Ni can be probed. This X-ray microscopy technique is therefore suitable for a wide range of studies: biological imaging in the water window[8,9]; studies of wet environmental samples[10,11]; studies of magnetic nanostructures with both elemental and spin-orbit sensitivity[12–14]; studies that require viewing through thin windows, coatings or substrates (such as buried electronic devices in a silicon chip[15]); and three-dimensional imaging of cryogenically fixed biological cells[9,16].

The microscope XM-1 at the Advanced Light Source (ALS) in Berkeley[17] is schematically shown in Fig. 1. The microscope type is similar to that pioneered by the Göttingen/BESSY group (ref. 18, and references therein). A 'micro' zone plate (MZP) projects a full-field image to an X-ray-sensitive CCD (charge-coupled device), typically in one or a few seconds, often with several hundred images per day. The field of view is typically 10 µm, corresponding to a magnification of 2,500. The condenser zone plate (CZP), with a central stop, serves two purposes in that it provides partially coherent hollow-cone illumination[2], and, in combination with a pinhole, serves as the monochromator. Monochromatic radiation of $\lambda/\Delta\lambda = 500$ is used. Both zone plates are fabricated in-house, using electron beam lithography[19].

The spatial resolution of a zone plate based microscope is equal to $k_1\lambda/\mathrm{NA}_{MZP}$, where λ is the wavelength, NA_{MZP} is the numerical aperture of the MZP, and k_1 is an illumination dependent constant, which ranges from 0.3 to 0.61. For a zone plate lens used at high magnification, $\mathrm{NA}_{MZP} = \lambda/2\Delta r_{MZP}$, where Δr_{MZP} is the outermost (smallest) zone width of the MZP[20]. For the partially coherent illumination[21,22] used here, $k_1 = 0.4$ and thus the theoretical resolution is $0.8\Delta_{MZP}$, as calculated using the SPLAT computer program[23] (a two-dimensional scalar diffraction code, which evaluates partially coherent imaging). In previous results with a $\Delta r_{MZP} = 25$ nm zone plate, we reported[2] an unambiguous spatial resolution of 20 nm. Here we describe the use of an overlay nanofabrication technique that allows us to fabricate zone plates with finer outer zone widths, to $\Delta r_{MZP} = 15$ nm, and to achieve a spatial resolution of below 15 nm, with clear potential for further extension.

This technique overcomes nanofabrication limits due to electron beam broadening in high feature density patterning. Beam broadening results from electron scattering within the recording medium (resist), leading to a loss of image contrast and thus resolvability for

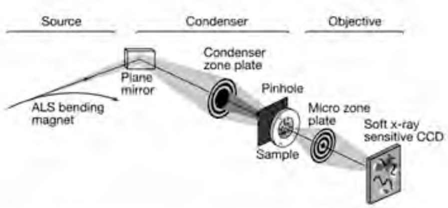

Figure 1 | A diagram of the soft X-ray microscope XM-1. The microscope uses a micro zone plate to project a full field image onto a CCD camera that is sensitive to soft X-rays. Partially coherent, hollow-cone illumination of the sample is provided by a condenser zone plate. A central stop and a pinhole provide monochromatization.

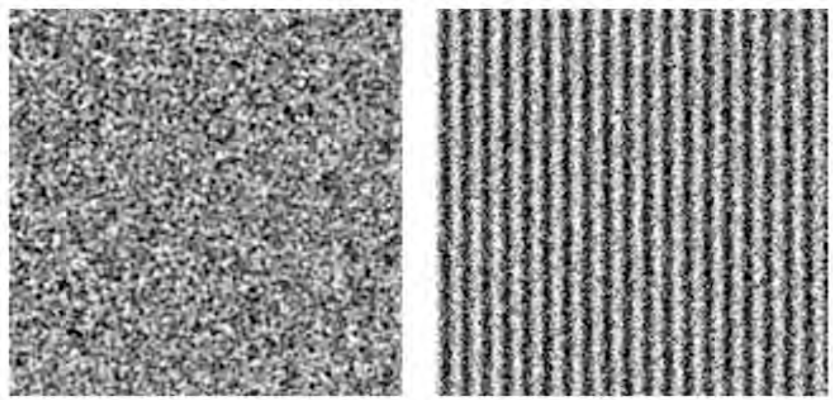

Figure 4 | Soft X-ray images of a 15.1 nm half-period test object, as formed with zone plates having outer zone widths of 25 nm and 15 nm.

Cr/Si test pattern (Cr L_3 @ 574 eV)
(2000 X 2000, 10^4 ph/pixel)

[1]Center for X-ray Optics, Lawrence Berkeley National Laboratory, 1 Cyclotron Road, MS 2-400. [2]Department of Electrical Engineering California, Berkeley, California 94720, USA.

Novel zone plates for specific functionality

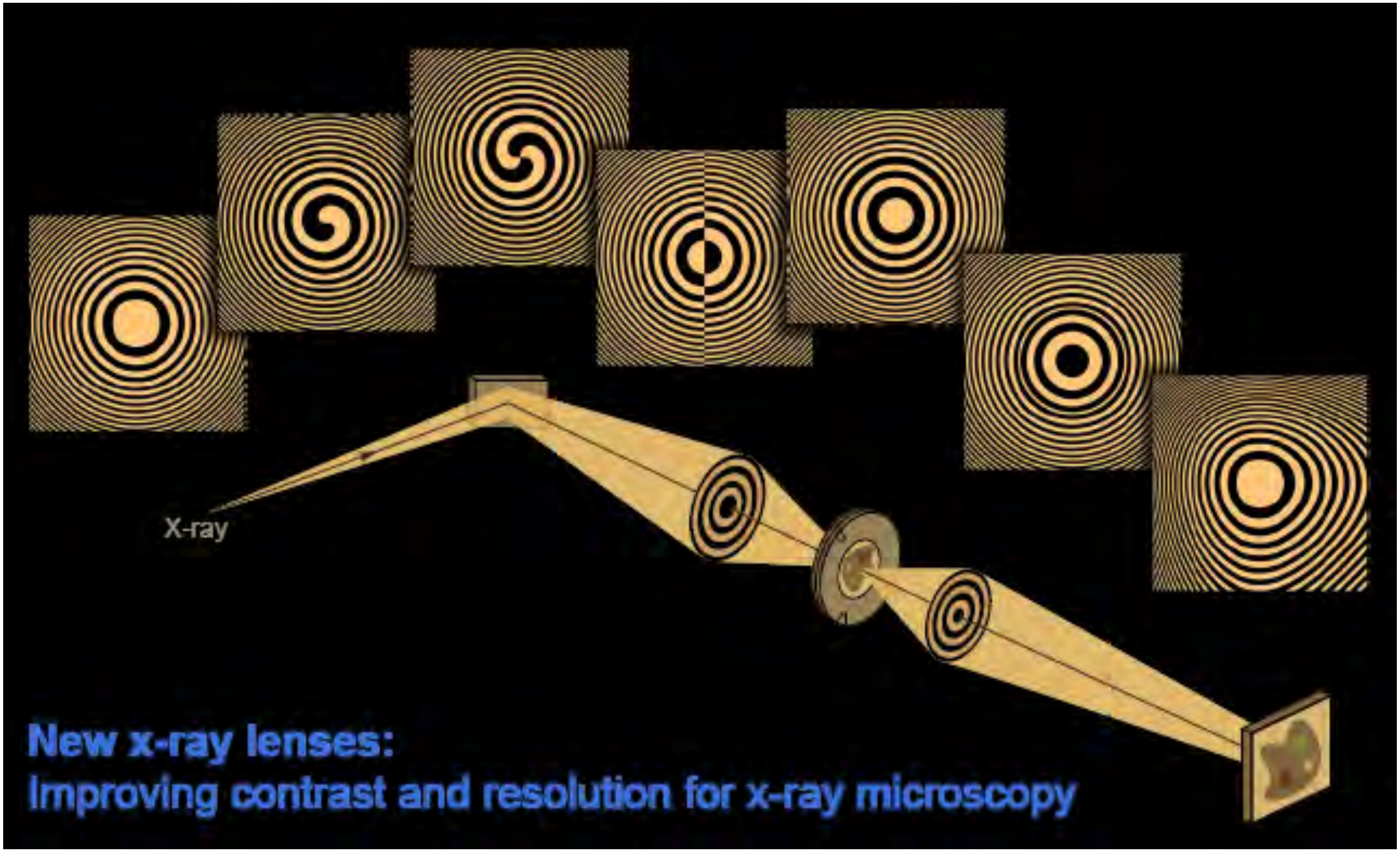

Courtesy of Anne Sakdinawat, UC Berkeley

High resolution zone plate microscopy

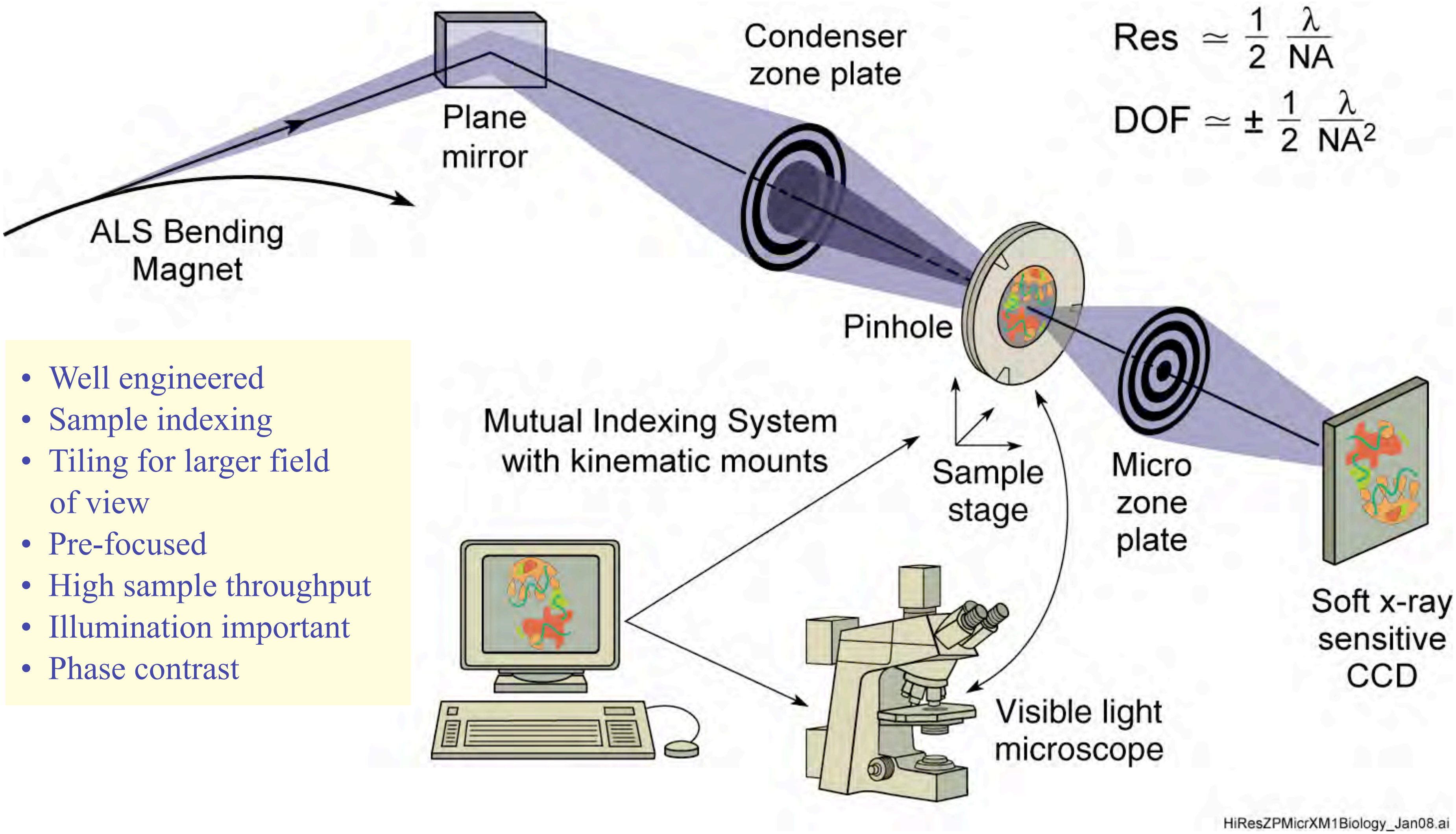

- Well engineered
- Sample indexing
- Tiling for larger field of view
- Pre-focused
- High sample throughput
- Illumination important
- Phase contrast

The water window for biological x-ray microscopy

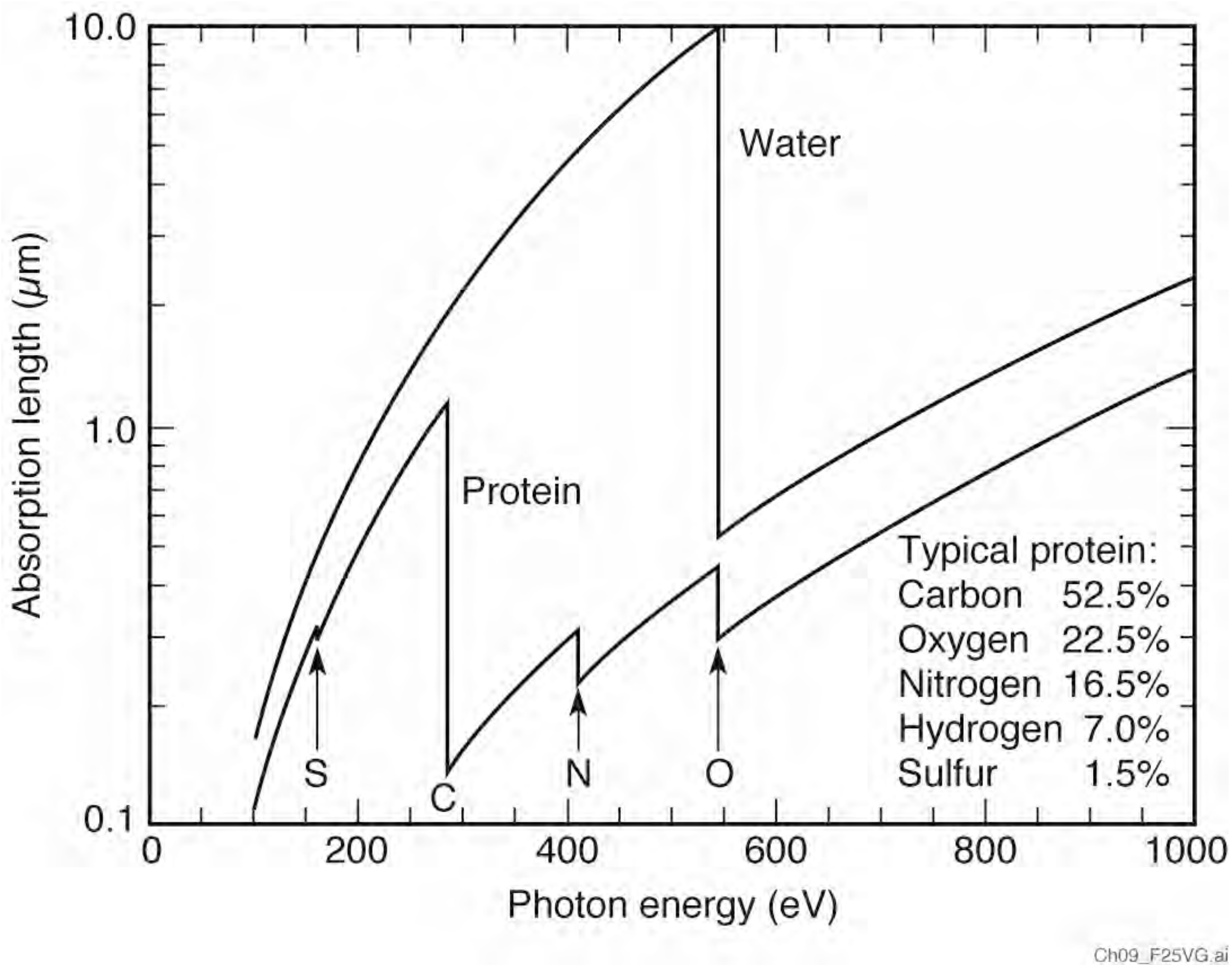

Fast freeze cryo fixation strongly mitigates radiation dose effects

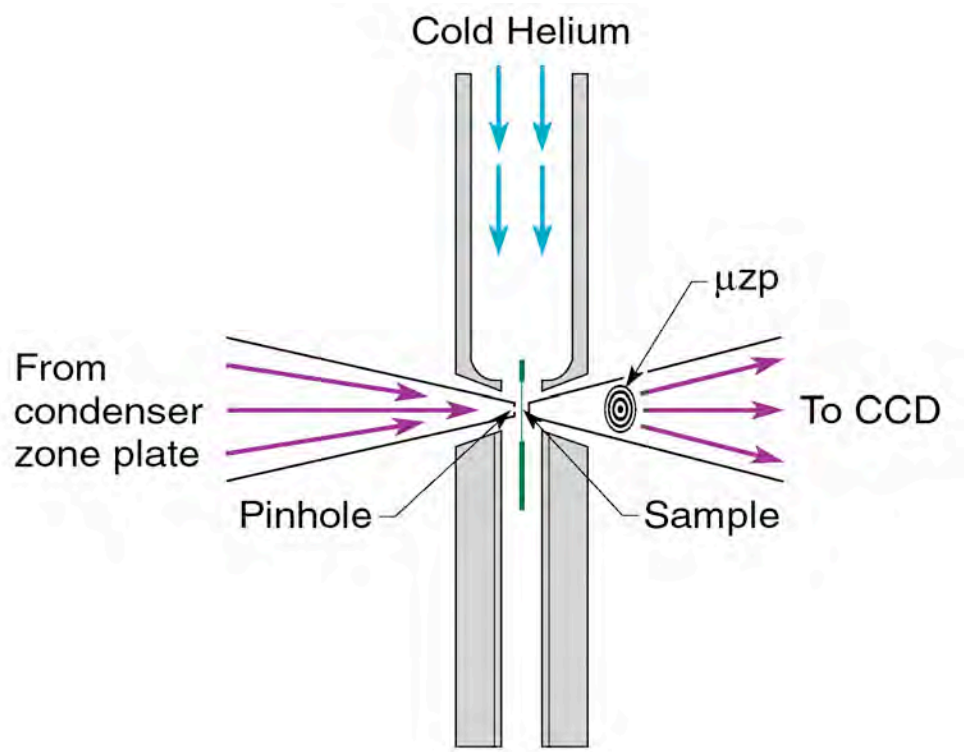

Helium passes through LN, is cooled, and directed onto sample windows

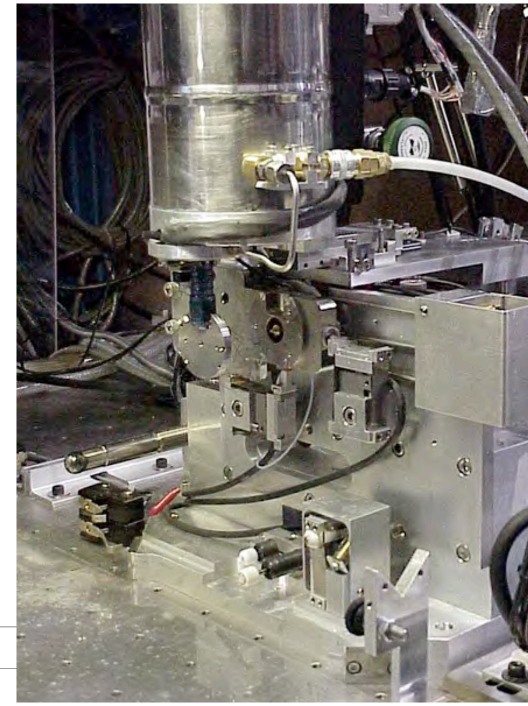

Fast Freeze

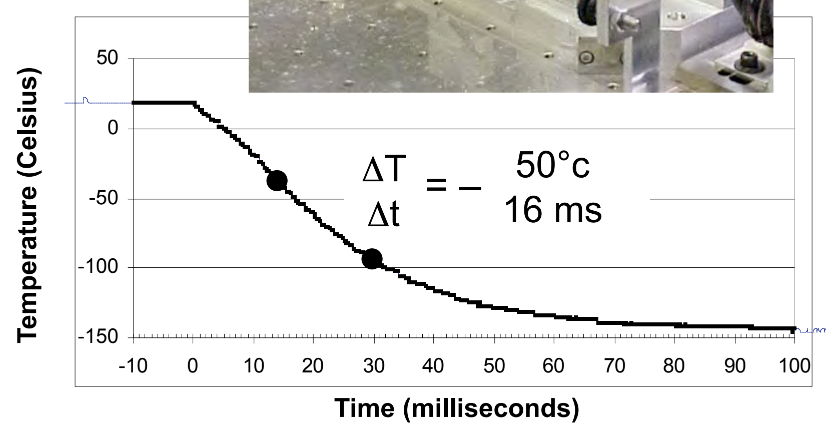

W. Meyer-Ilse, G. Denbeaux, L. Johnson, A. Pearson (CXRO-LBNL)

Organelle details imaged with cryogenic preservation and high spatial resolution

Cryo x-ray microscopy of 3T3 fibroblast cells

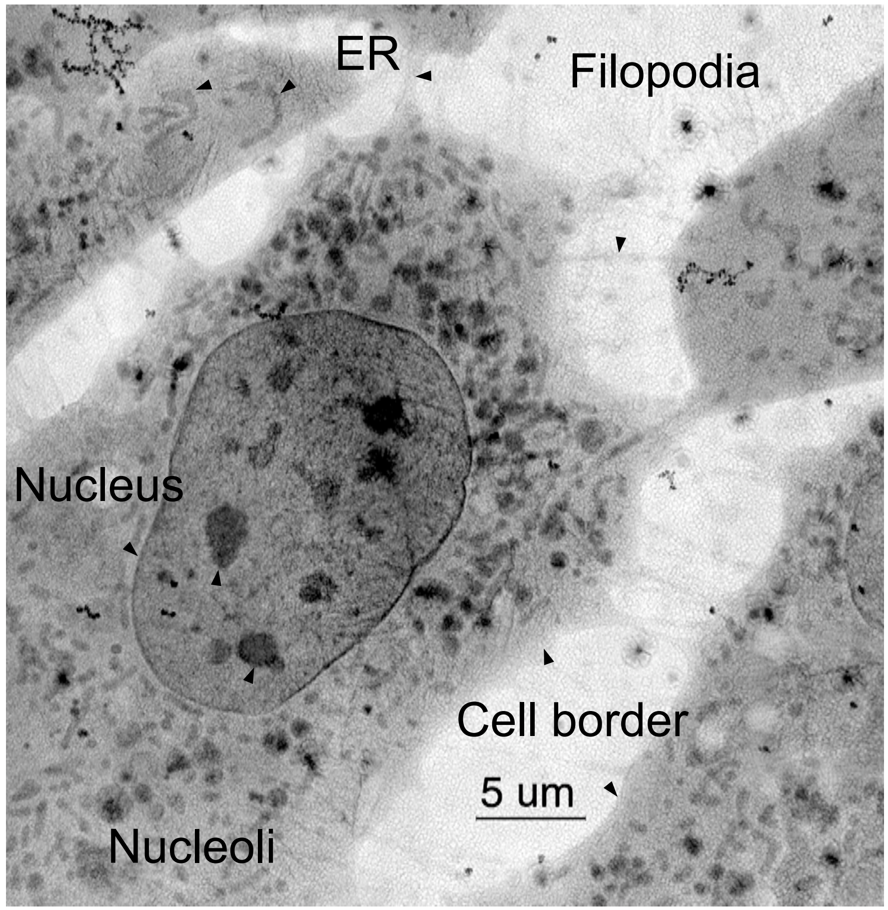

C. Larabell, D. Yager, D. Hamamoto, M. Bissell, T. Shin (LBNL Life Sciences Division)
W. Meyer-Ilse, G. Denbeaux, L. Johnson, A. Pearson (CXRO-LBNL)

Bending magnet radiation used with a soft x-ray microscope to form a high resolution image of a whole, hydrated mouse epithelial cell

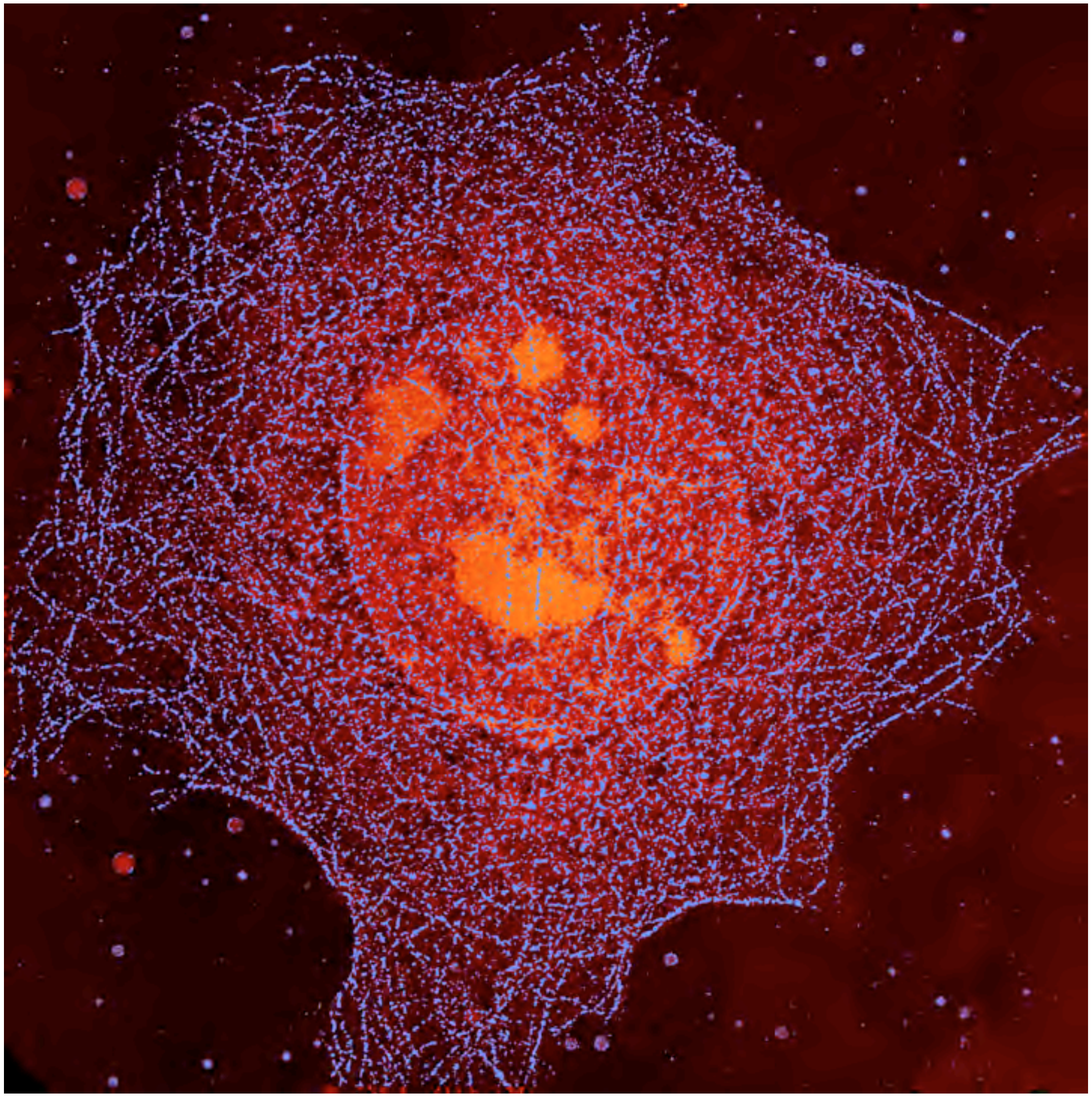

Courtesy of C. Larabell and W. Meyer-Ilse (LBNL)

*h*w = 520 eV

32 µm x 32 µm

Ag enhanced Au labeling of the microtubule network, color coded blue.

Cell nucleus and nucleoli, moderately absorbing, coded orange.

Less absorbing aqueous regions coded black.

W. Meyer-Ilse et al.
J. Microsc. 201, 395 (2001)

Bio-nanotomography for 3D imaging of cells

Nanotomography of Cryogenic Fixed Cells

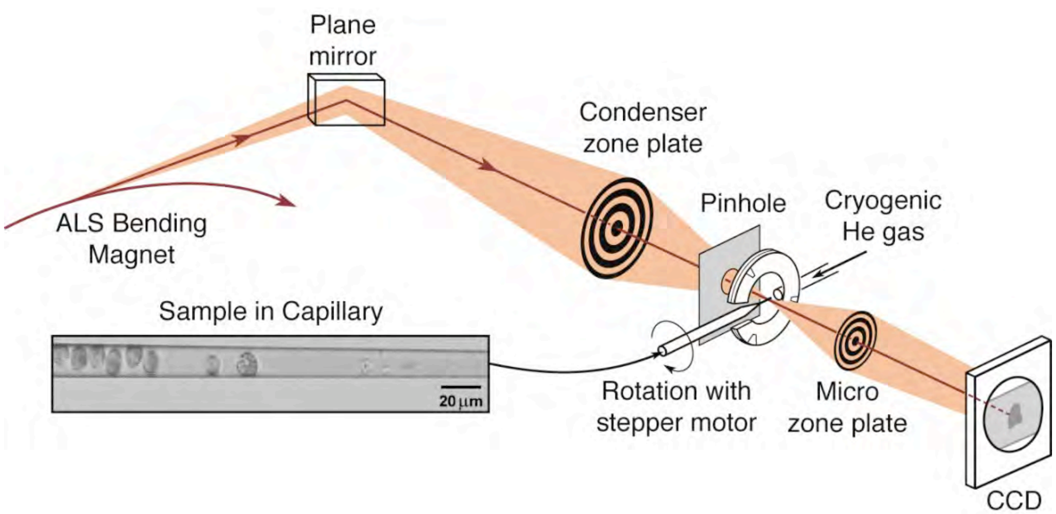

Courtesy of G. Schneider (BESSY)
Surf. Rev. Lett. 9, 177 (2002)

Soft X-Ray Nanotomography of a Yeast Cell

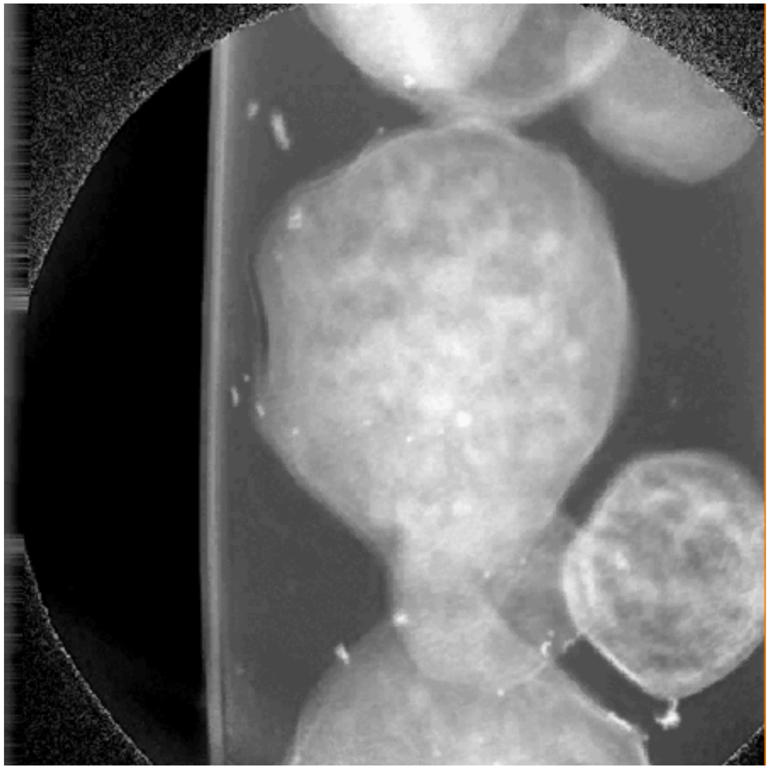

$\lambda = 2.4$ nm

Courtesy of C. Larabell (UCSF & LBNL) and M. LeGros (LBNL)

UCSF NCXT

Bio-nanotomography for 3D imaging of cells

Nanotomography of Cryogenic Fixed Cells

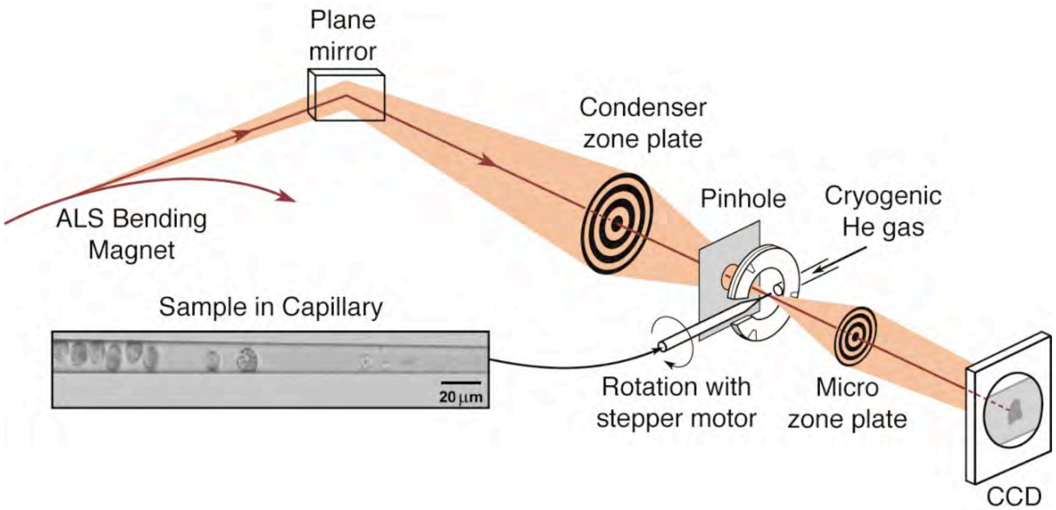

λ = 2.4 nm (517 eV)
Δr = 35 nm
N = 320
NA = 0.034
D = 45 µm
f = 650 µm
σ = 0.64
Resolution = 60 nm

Soft X-Ray Nanotomography of a Yeast Cell

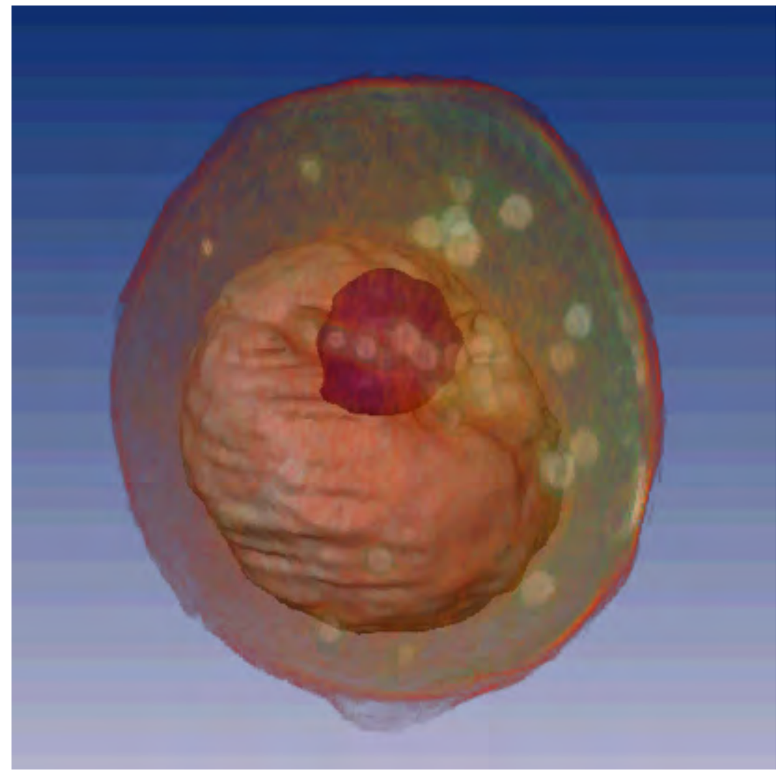

λ = 2.4 nm

Courtesy of C. Larabell (UCSF & LBNL) and M. LeGros (LBNL)

Nanoscale 3-D biotomography

Mother daughter yeast cells just before separation

2-D slice from 3-D Tomogram. Images every 2°, 180° data set, several minutes. Δr = 45 nm

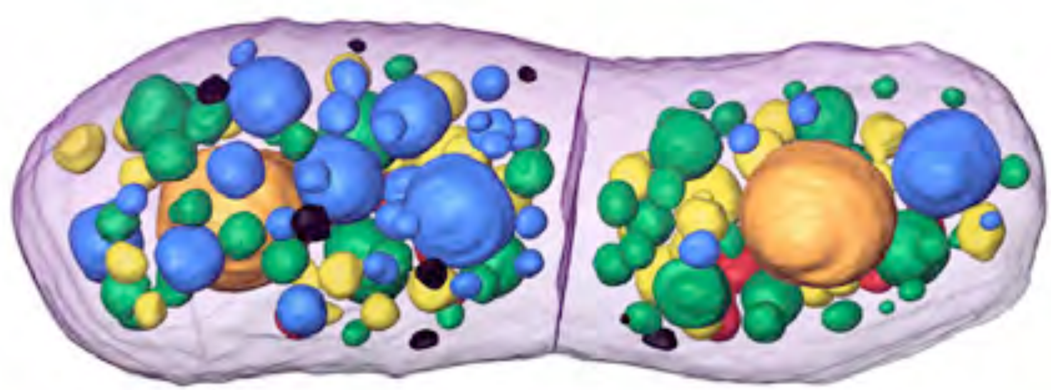

Color coding identifies subcellular components by their x-ray absorption coefficients

Courtesy of Carolyn Larabell, UCSF/LBNL.

Applications of soft x-ray microscopy

Biotomography at 60 nm resolution

- Cryofixation
- 2° angular intervals
- Depth of focus limits resolution
- New XM-2 dedicated to biological applications, will become major facility worldwide to draw biologists to this evolving capability

Courtesy of C. Larabell (UCSF & LBNL)

UCSF NCXT

Magnetic x-ray microscopy using x-ray magnetic circular dichroism (XMCD)

Magnetic X-Ray Microscopy

- **High spatial resolution in transmission**
- **Bulk sensitive (thin films)**
- **Complements surface sensitive PEEM**
- **Good elemental sensitivity**
- **Good spin-orbit sensitivity**
- **Allows applied magnetic field**
- **Insensitive to capping layers**
- **In-plane and out-of-plane measurements**

100 nm
lines &
spaces

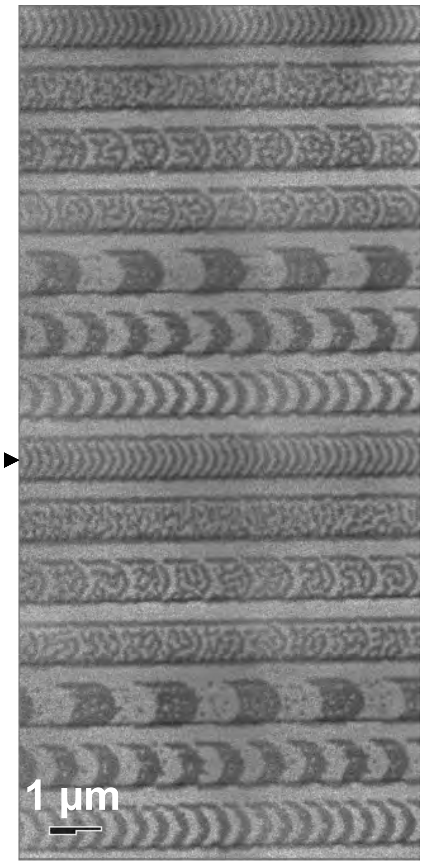

Courtesy of P. Fischer, (MPI, Stuttgart) and G. Denbeaux (CXRO/LBNL)

Magnetic domains imaged at different photon energies

FeGd Multilayer

Contrast reversal

1 µm

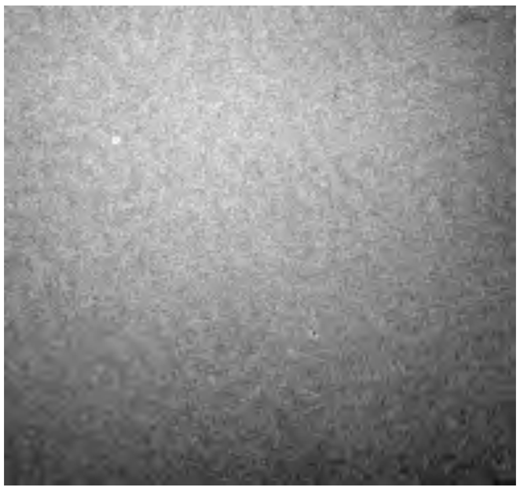

$\hbar\omega$ = 704 eV
below Fe L-edges

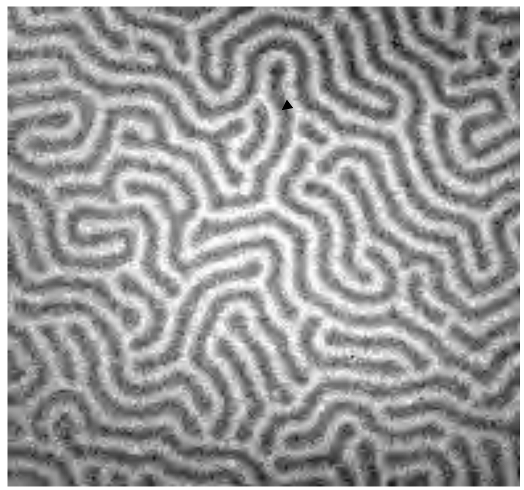

$\hbar\omega$ = 707.5 eV
Fe L_3-edge

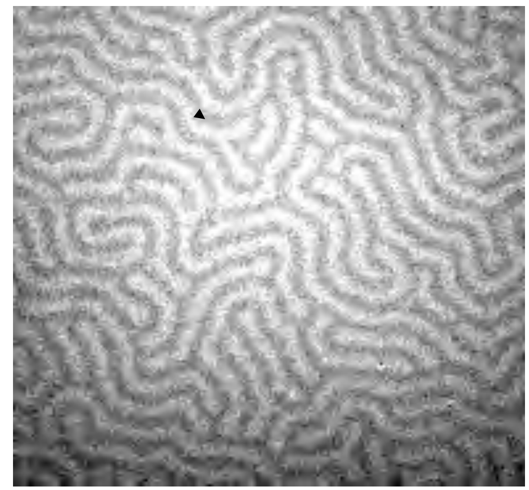

$\hbar\omega$ = 720.5 eV
Fe L_2-edge

P. Fischer, T. Eimueller, M. Koehler (U. Wuerzberg)
S. Tsunashima (U. Nagoya) and N. Tagaki (Sanyo)
G. Denbeaux, L. Johnson, A. Pearson (CXRO-LBNL)

Magnetic recording of nanomagnetic patterns to 15 nm spatial resolution

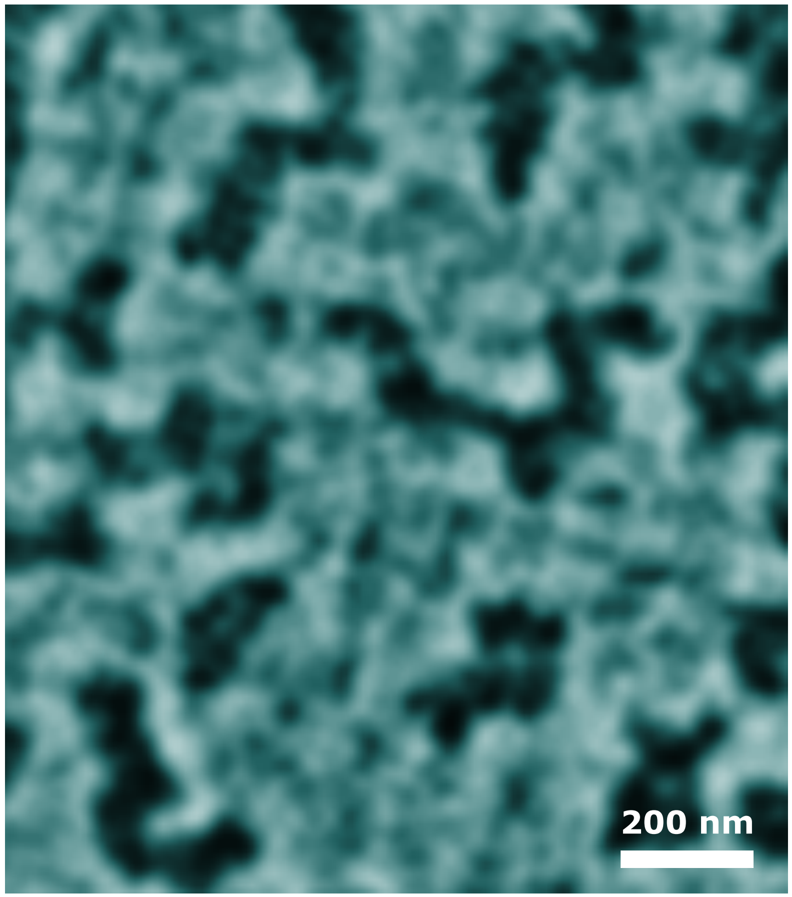

Courtesy of Peter Fischer (LBNL)

CoCrPt alloy
Co L_3-edge at 778 eV
(1.59 nm)

P. Fischer et al., *Mat. Today* 9, 26 (2006).

Time resolved studies of vortex dynamics in patterned permalloy thin films

Pump and Probe setup requires:

- Pump: Current pulse to “pump” sample
- Probe: X-ray pulses (70ps) from ALS 2 Bunch mode
- Perfect repeatability of dynamics

<u>Sample:</u>

50 nm thick 2μmx4μm permalloy ($Ni_{80}Fe_{20}$)

100nm thick gold waveguide

(ΔI along waveguide generates field to pump sample)

B.L. Mesler, P. Fischer,W. Chao, E. H. Anderson, D.H. Kim J. Vac. Sci. Technol. B 25, 2598 (2007).

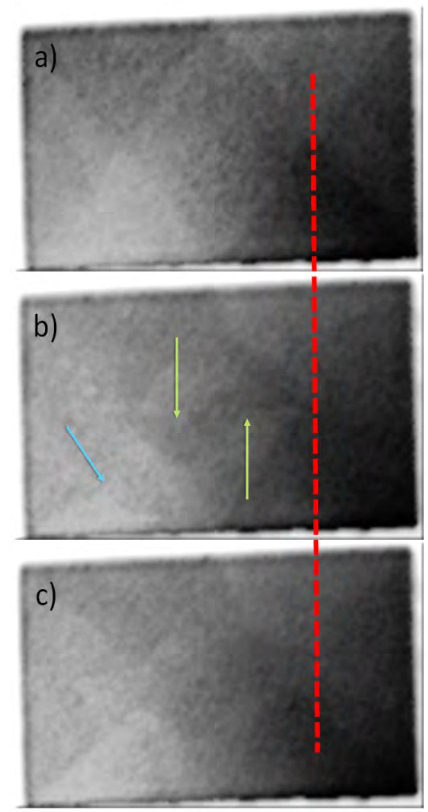

Environmental Consequences of Portland cement

1.5 billion ton of cement

Problem!

- **Generates 1.5 billion ton of CO_2**
- **Responsible for 7% CO_2 production in the world**

Courtesy of Professor Paulo Monteiro, CEE, UC Berkeley

Nanoscale x-ray imaging of cement processes: early hydrates forming during the pre-induction period

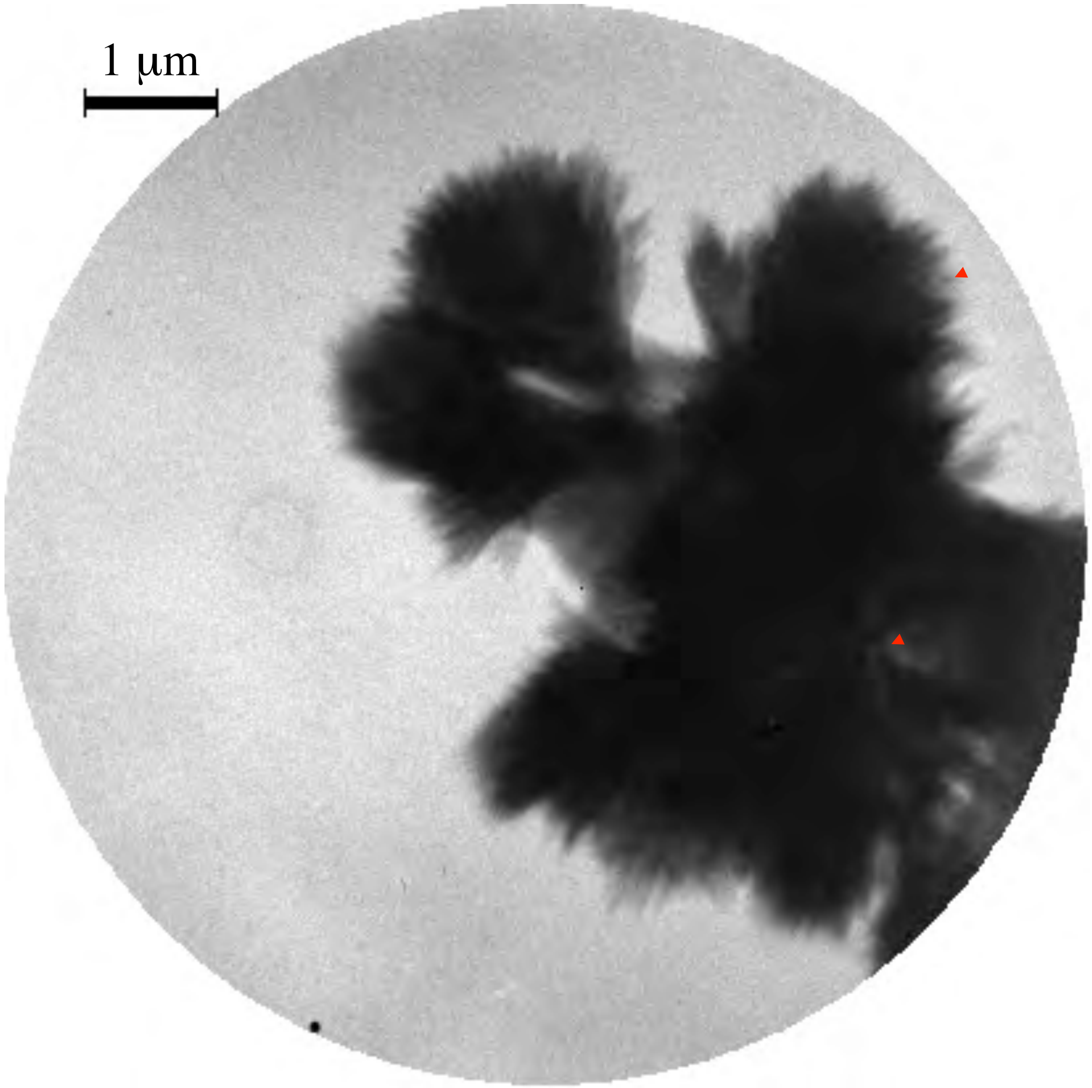

Early hydrates (Sheaf of wheat)

Grain

C3S hydrated for 34 min. in saturated lime and calcium sulfate at w/c = 5, 1 s exposure time, 516 eV, scale bar 1μm.

Courtesy of Professor Paulo Monteiro, CEE, UC Berkeley

Nanoscale x-ray imaging of cement processes

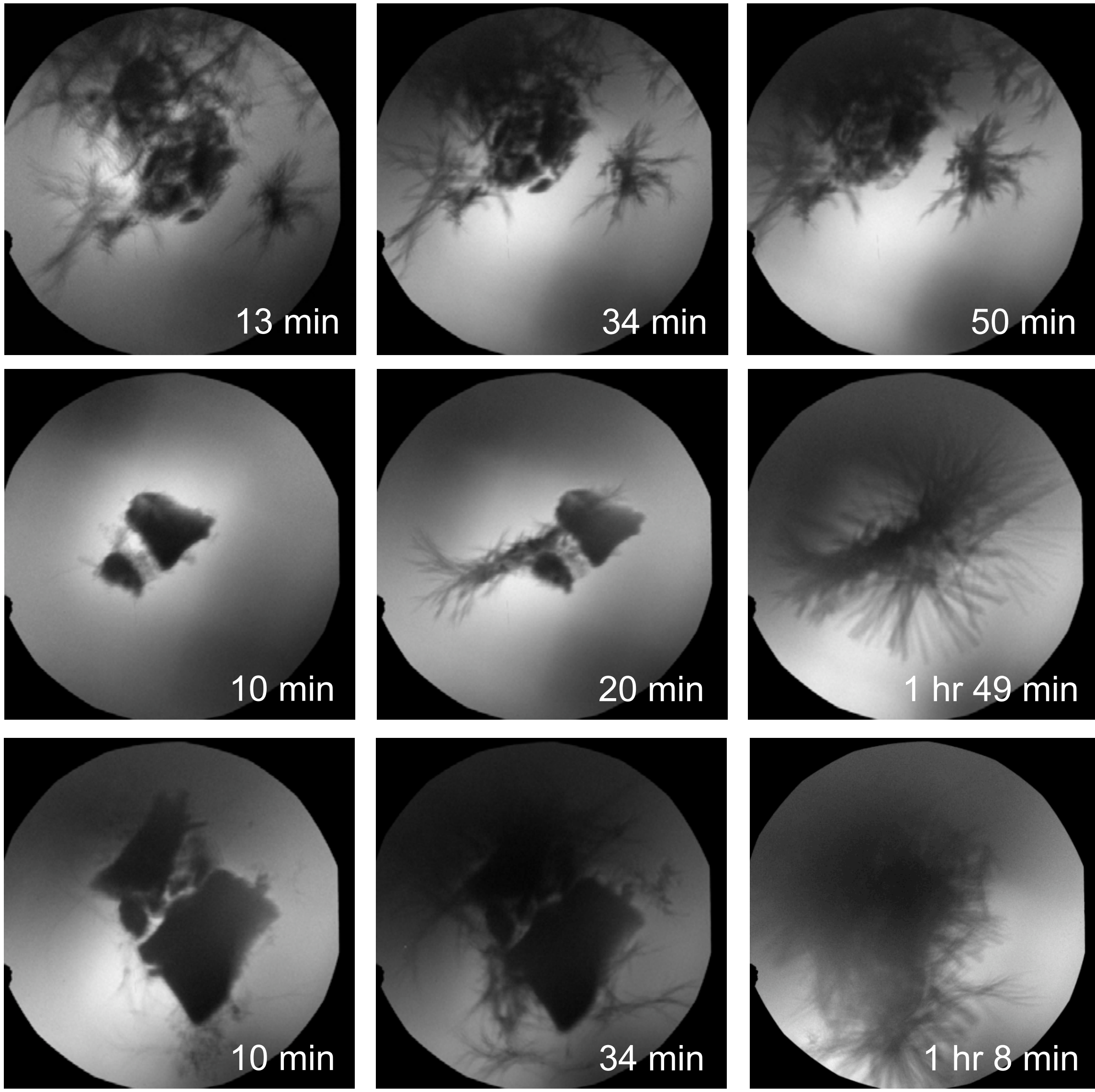

Orth C_3A

Orth C_3A + 1% $CaCl_2$

Orth C_3A + accelerator

C: carbon
Ca: calcium
A: alumina (Al_2O_3)
S: silica (SiO_2)

520 eV, 40 nm – spatial resolution

Courtesy of Professor Paulo Monteiro, CEE, UC Berkeley

Spectromicroscopy: high spatial and high spectral resolution of surface and thin films

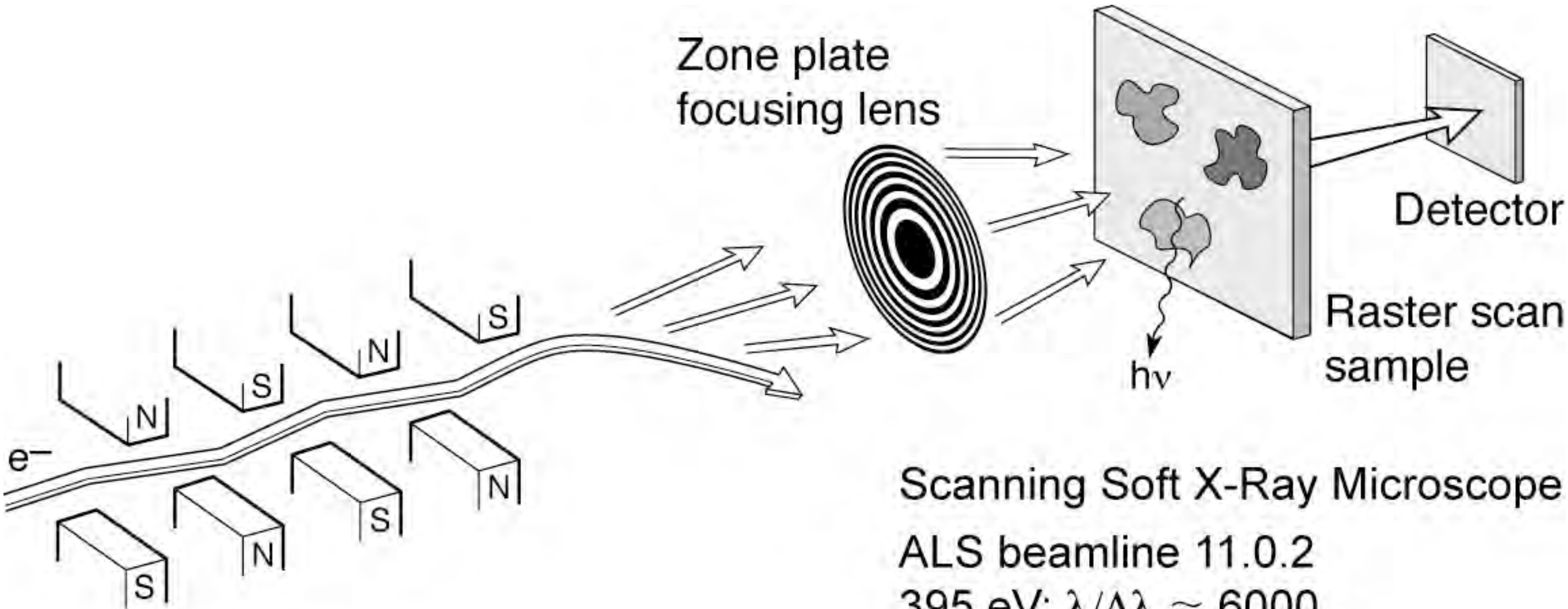

Scanning Soft X-Ray Microscope

ALS beamline 11.0.2

395 eV; $\lambda/\Delta\lambda \simeq 6000$

240 × 240 pixels

1.2 μm × 1.2 μm

2 ms dwell time

Ch09_F40a_Feb2010.ai

Biofilm from Saskatoon River

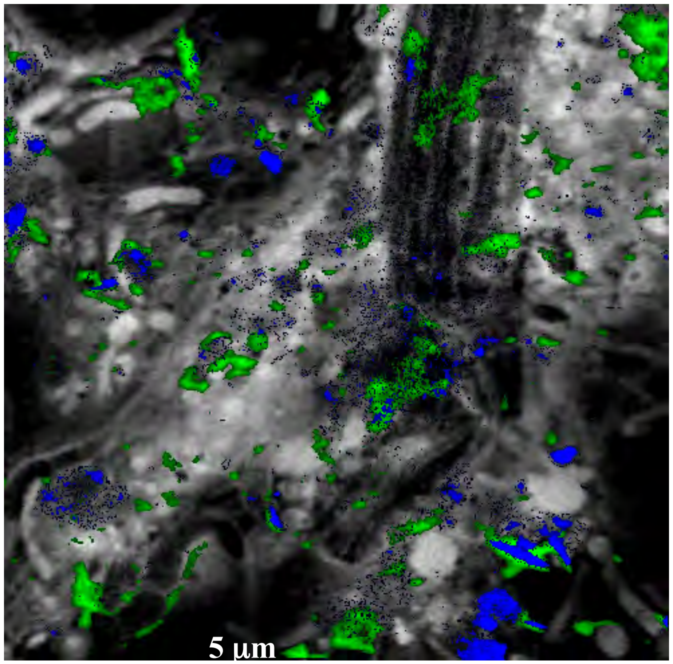

Protein (gray), Ca, K

RESULTS
•Ni, Fe, Mn, Ca, K, O, C elemental map, (there was no sign of Cr.)
•Different oxidation states for Fe and Ni

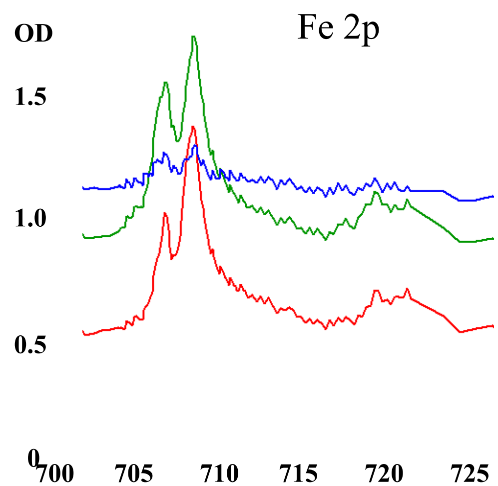

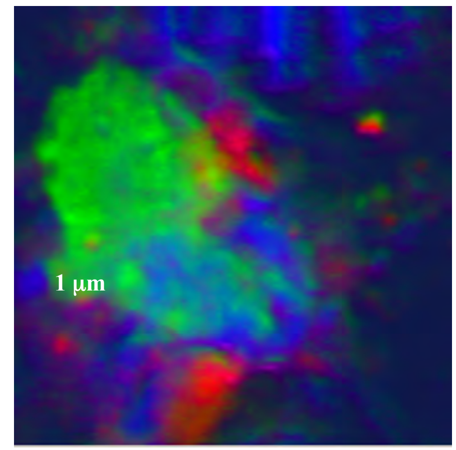

Different oxidation states (minerals) found for Fe & Ni

Tohru Araki, Adam Hitchcock (McMaster University)
Tolek Tyliszczak, LBNL
Sample from: John Lawrence, George Swerhone (NWRI-Saskatoon), Gary Leppard (NWRI-CCIW)

Patterned polymer photoresists

ALS-MES 11.0.2

M.K. Gilles, R. Planques, S.R. Leone
LBNL
Samples from B. Hinsberg, F. Huele
IBM Almaden

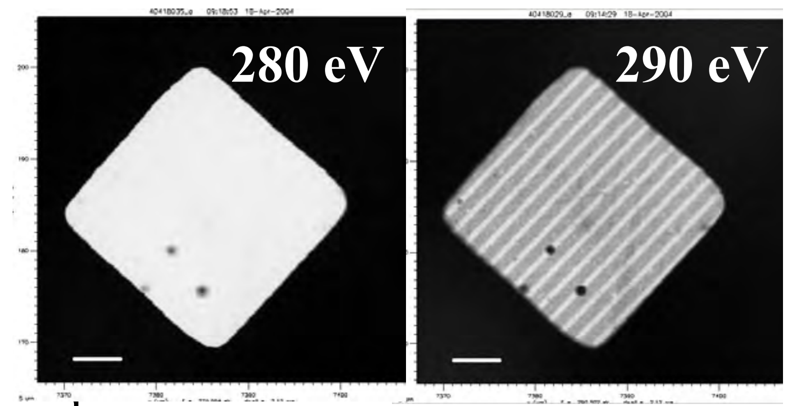

Exposure to UV light results in loss of carbonyl peak

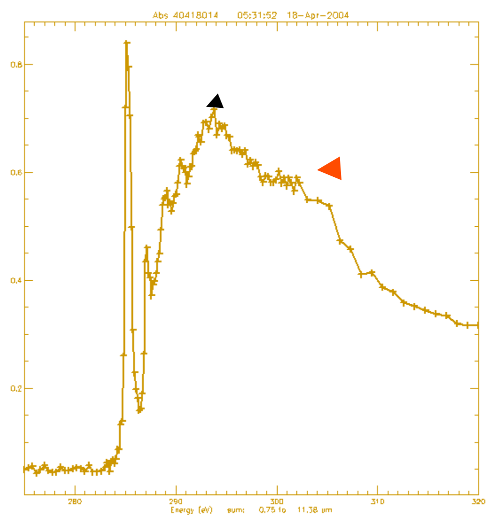

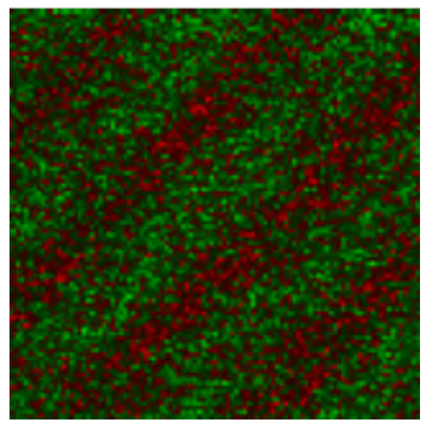

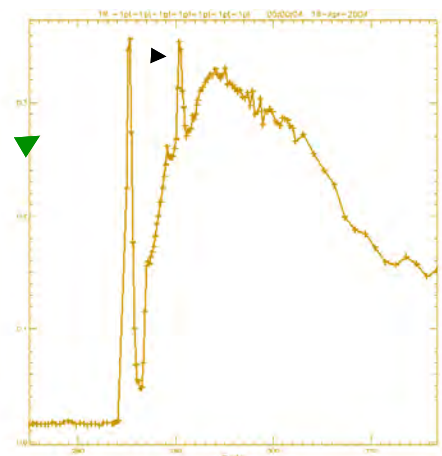

Map chemical spectra taken of pure samples onto a sample containing both components

Courtesy of Mary Gilles, LBNL

Hard x-ray zone plate microscopy

- Shorter wavelengths, potentially better spatial resolution and greater depth-of-field.
- Less absorption (β); phase shift (δ) dominates, higher efficiency.
- Thicker structures required (e.g., zones), higher aspect ratios pose nanofabrication challenges.
- Contrast of nanoscale samples minimal; will require good statistics, uniform background, dose mitigation.

nanoXCT: Schematic and Challenges

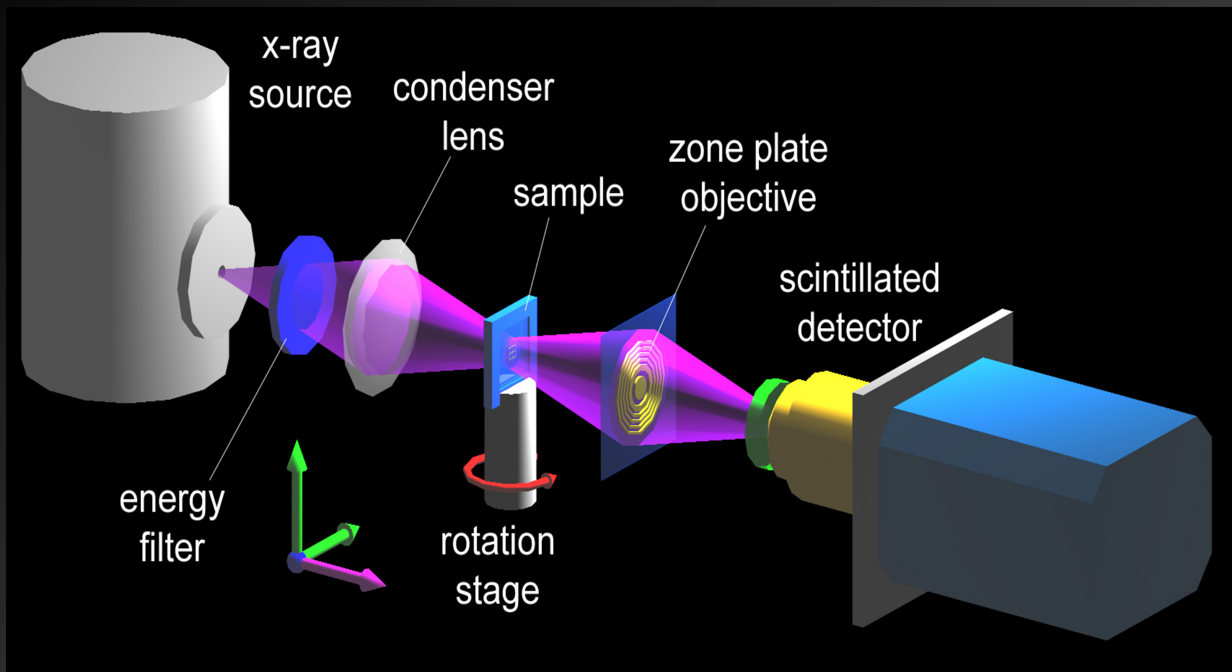

X-ray Zone-plate Lens

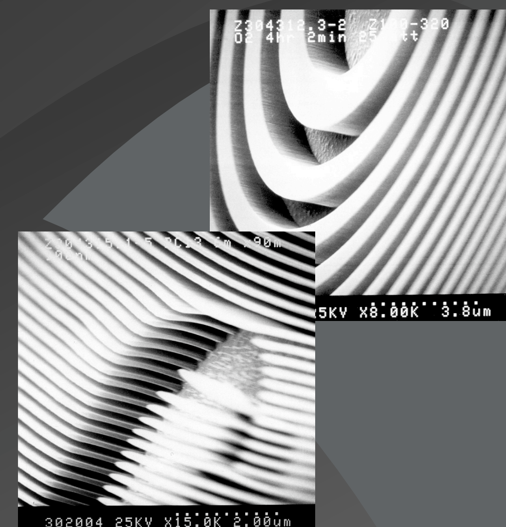

Challenges for achieving nm scale resolution:

- High resolution objective lens: limiting the ultimate resolution
- High numerical aperture condenser lens:
- Detector: high efficiency for lab. source and high speed for synchrotron sources
- Precision mechanical system

Courtesy of Wenbing Yun and Michael Feser, Xradia

Xradia nanoXCT: Sub-25 nm Hard X-ray Image

Xradia Resolution Pattern
- 50 nm bar width
- 150 nm thick Au
- 8keV x-ray energy
- 3rd diffraction order

F. Duewer, M. Tang,
G. C. Yin, W. Yun,
M. Feser, et al.

Xradia nano-XCT
8-50S installed at
NSRRC, Taiwan

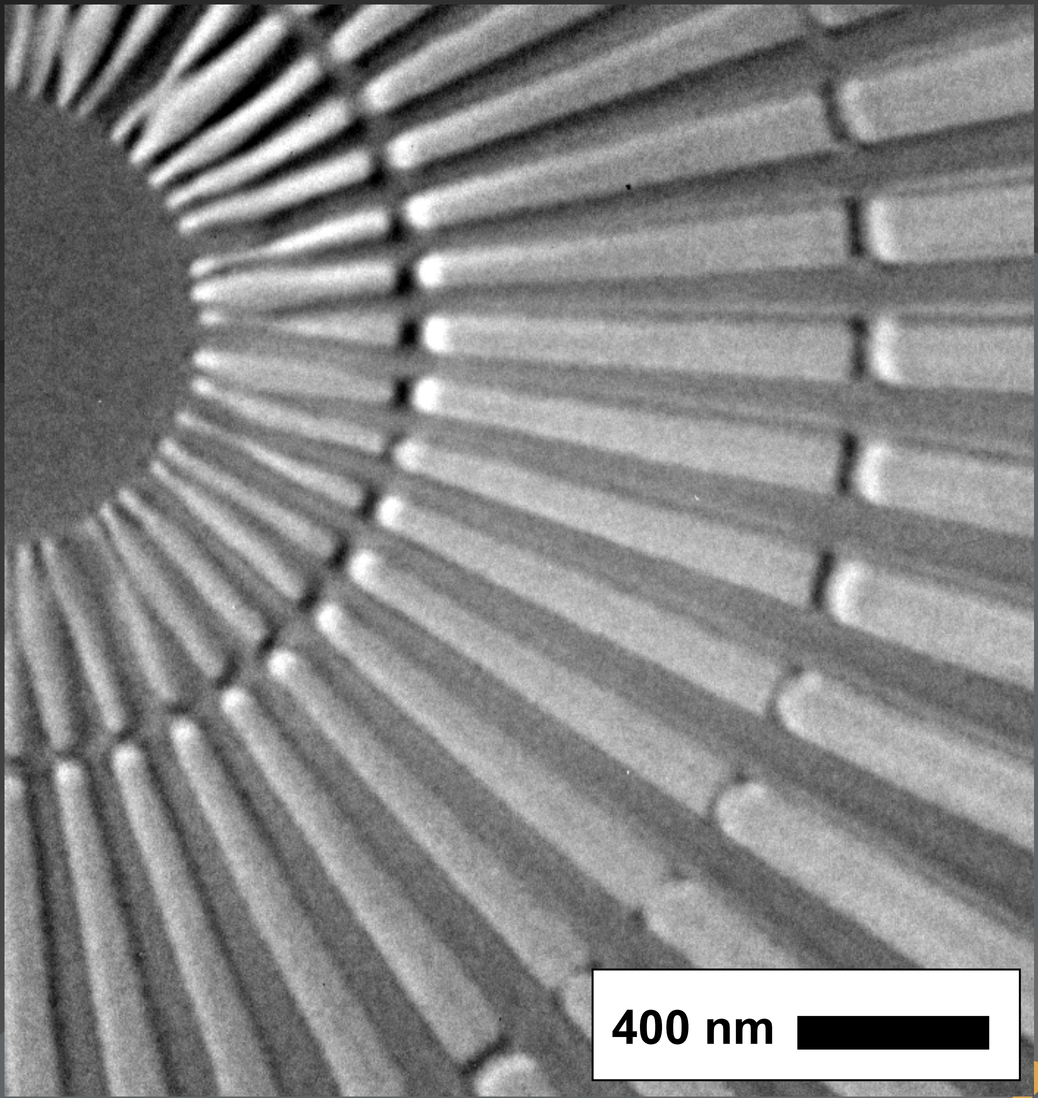

Elemental contrast by tuning energy across the copper absorption edge (Guan-Chian Yin *et al*)

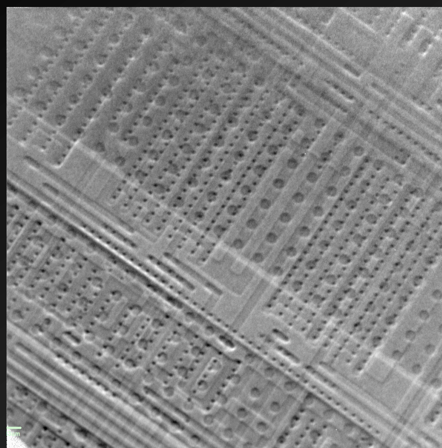

8.4 keV

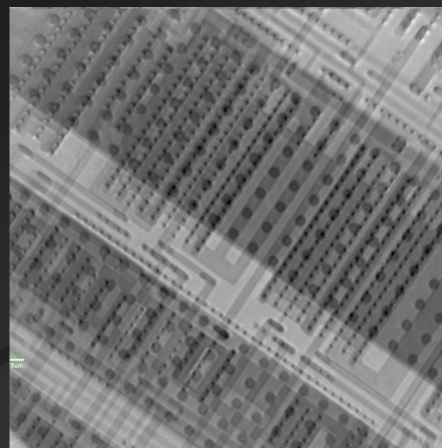

9.5 keV

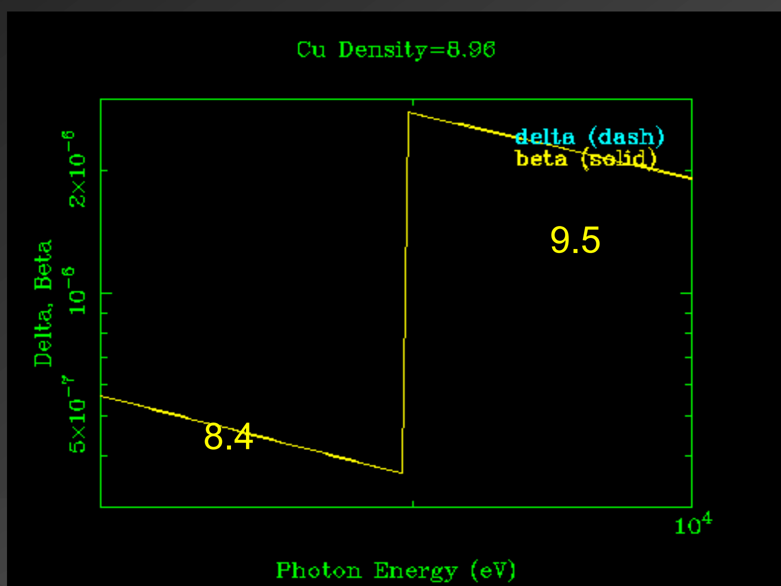

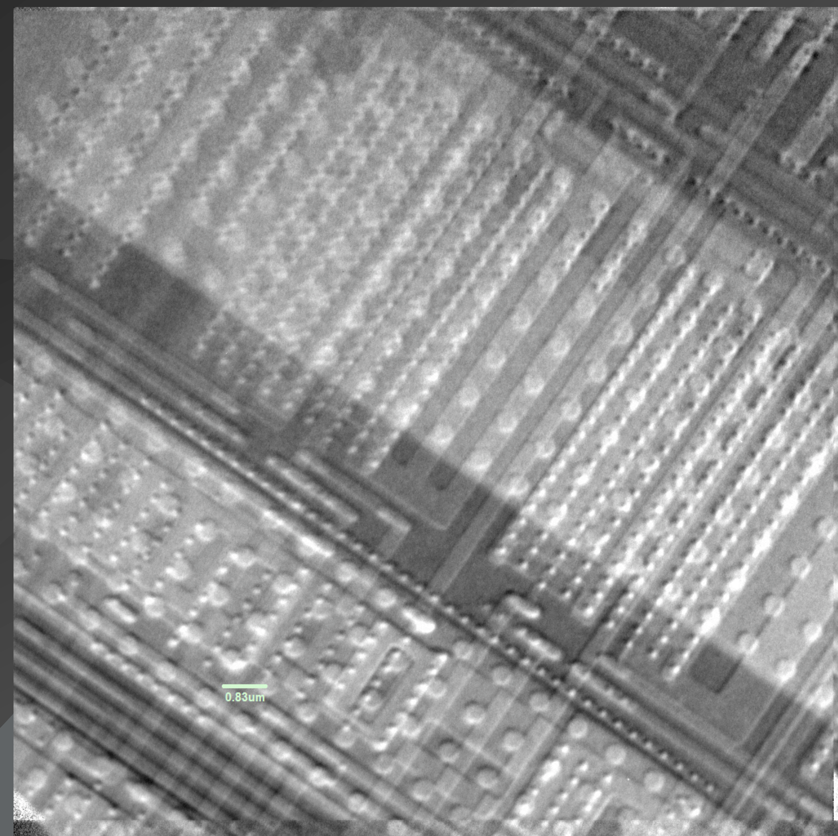

Intensity difference between
E = 8.4 keV and 9.5 keV

Tomography of a Tungsten plug with "keyhole" at ~60 nm spatial resolution

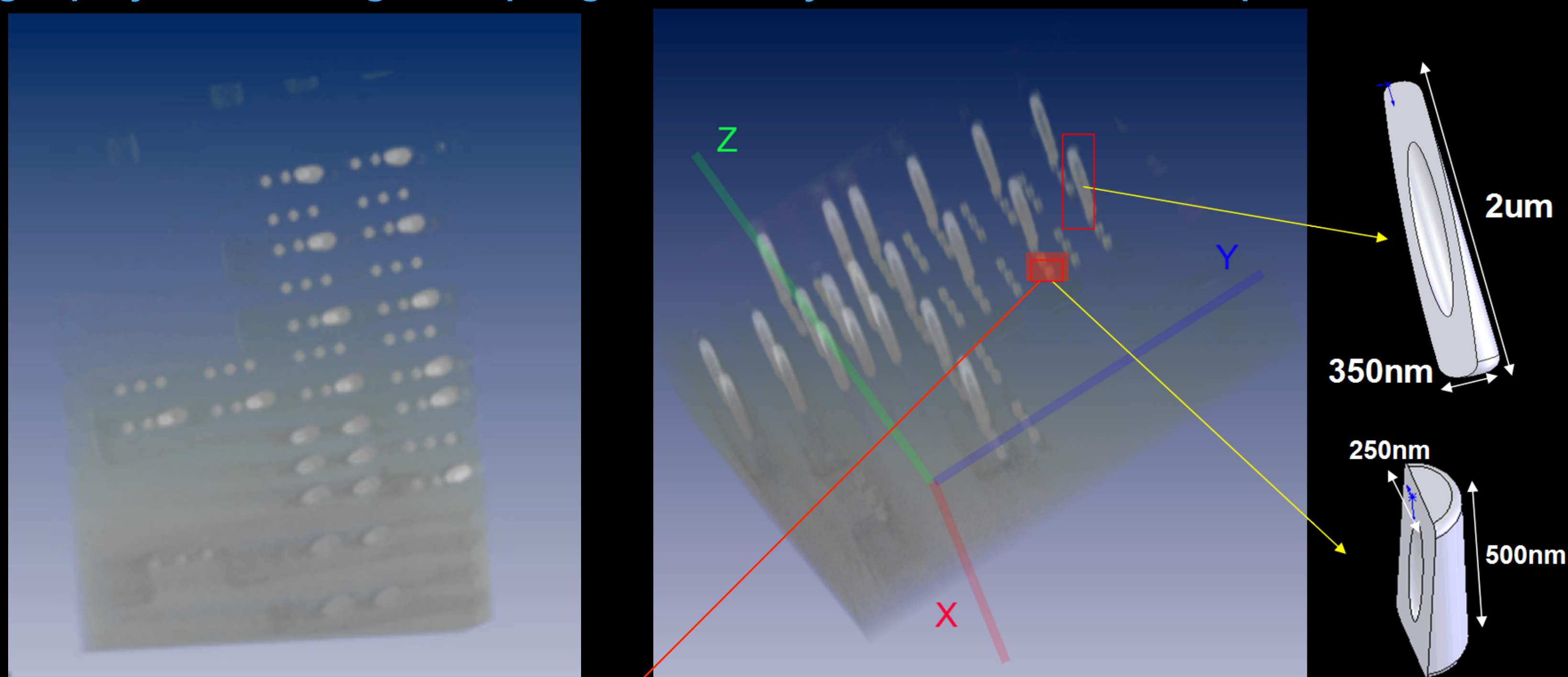

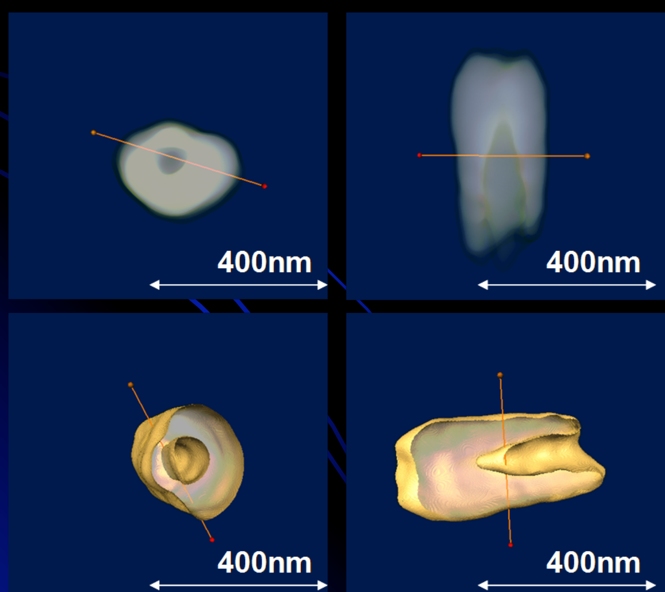

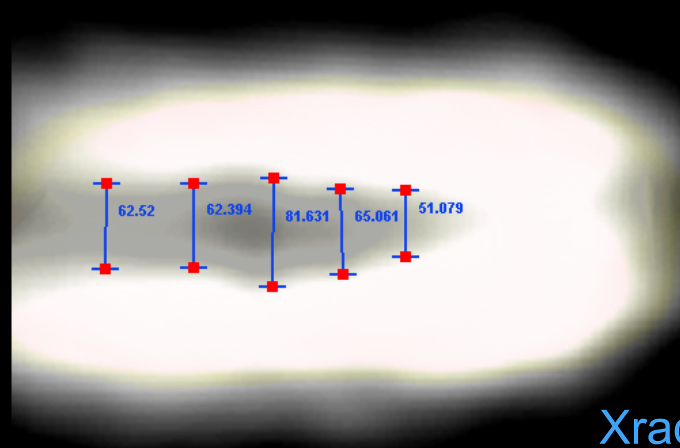

Xradia and NSRRC

APL. 88, 241115 (2006)

Scanning x-ray fluorescence microprobe (μ-XRF)

Kirkpatrick-Baez (KB) mirror pair

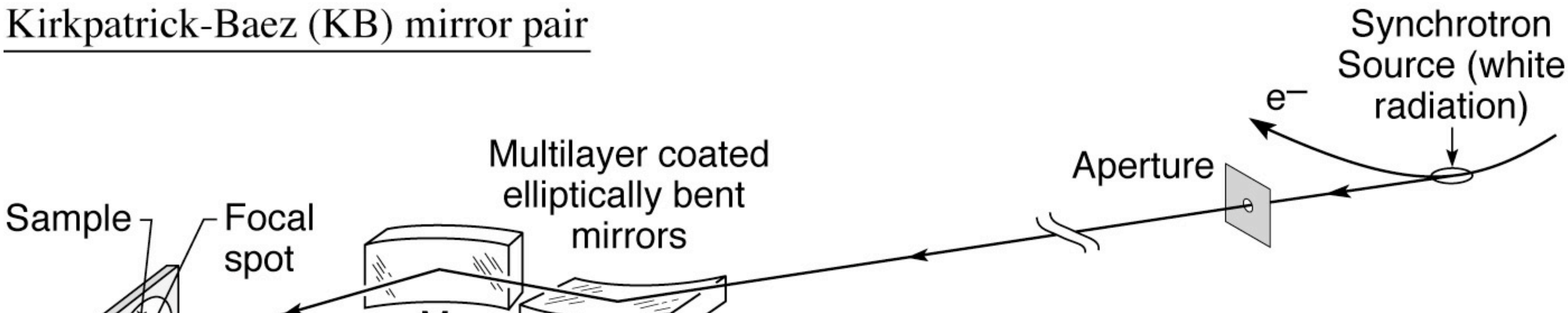

- Crossed cylinders at glancing incidence
- Photon in / photon out, low noise background
- Femtogram and part per billion (ppb) sensitivity
- Micron focus (1988), now ~25 nm (Yamauchi, Mimura and colleagues, Osaka U./SPring-8)

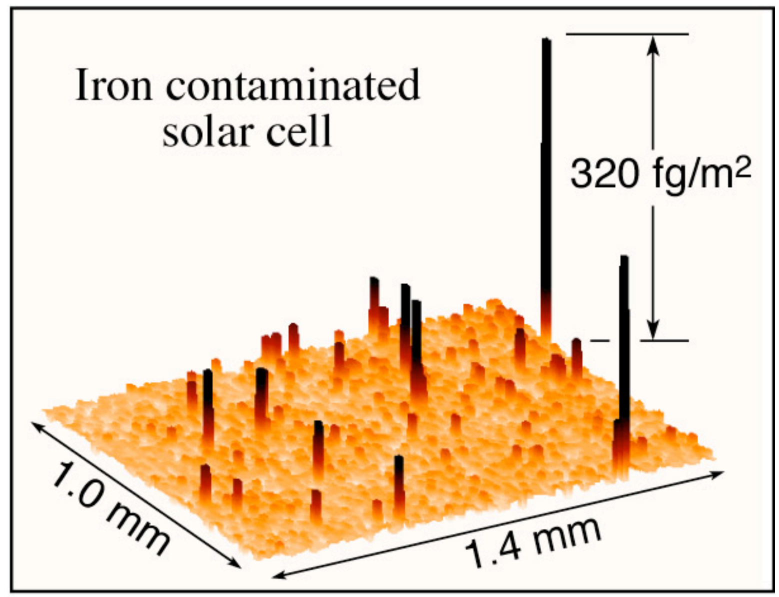

(Courtesy of A. Thompson and J. Underwood, LBNL; and R. Holm, Miles Lab)

FluoresMicroprobe_Sept2010.ai

J.H. Underwood and A.C. Thompson, NIM A266, 296 & 318 (1988).

X-ray microprobe at SPring-8

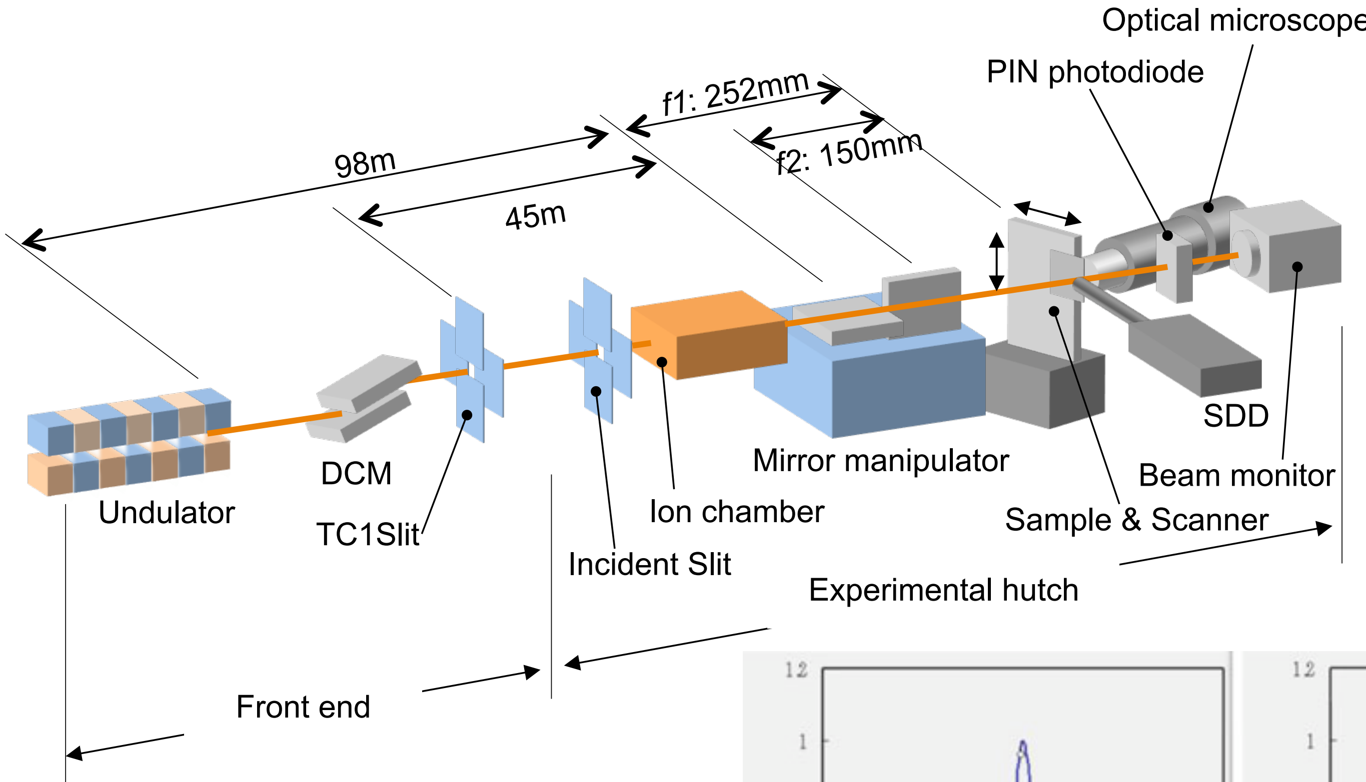

S. Matsuyama et al.,
Rev. Sci. Instrum.
77, 103102 (2006)

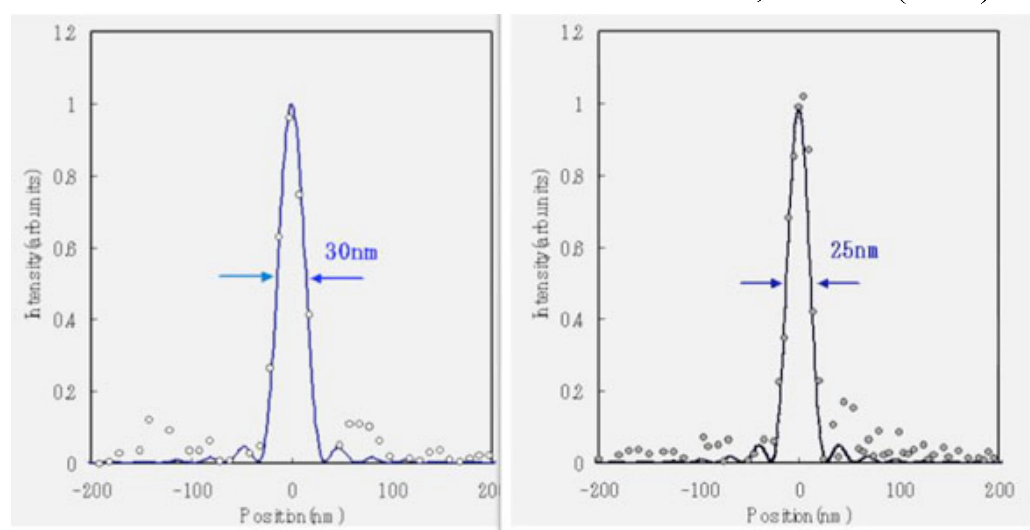

Courtesy of K. Yamauchi and
H. Mimura, Osaka University.

Sub-cellular elemental analysis using the hard x-ray fluorescence microprobe at SPring-8

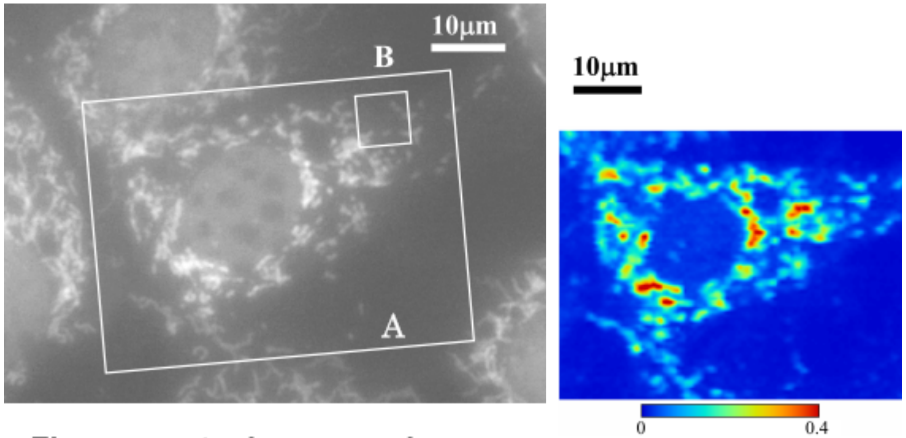

Fluorescent microscope image

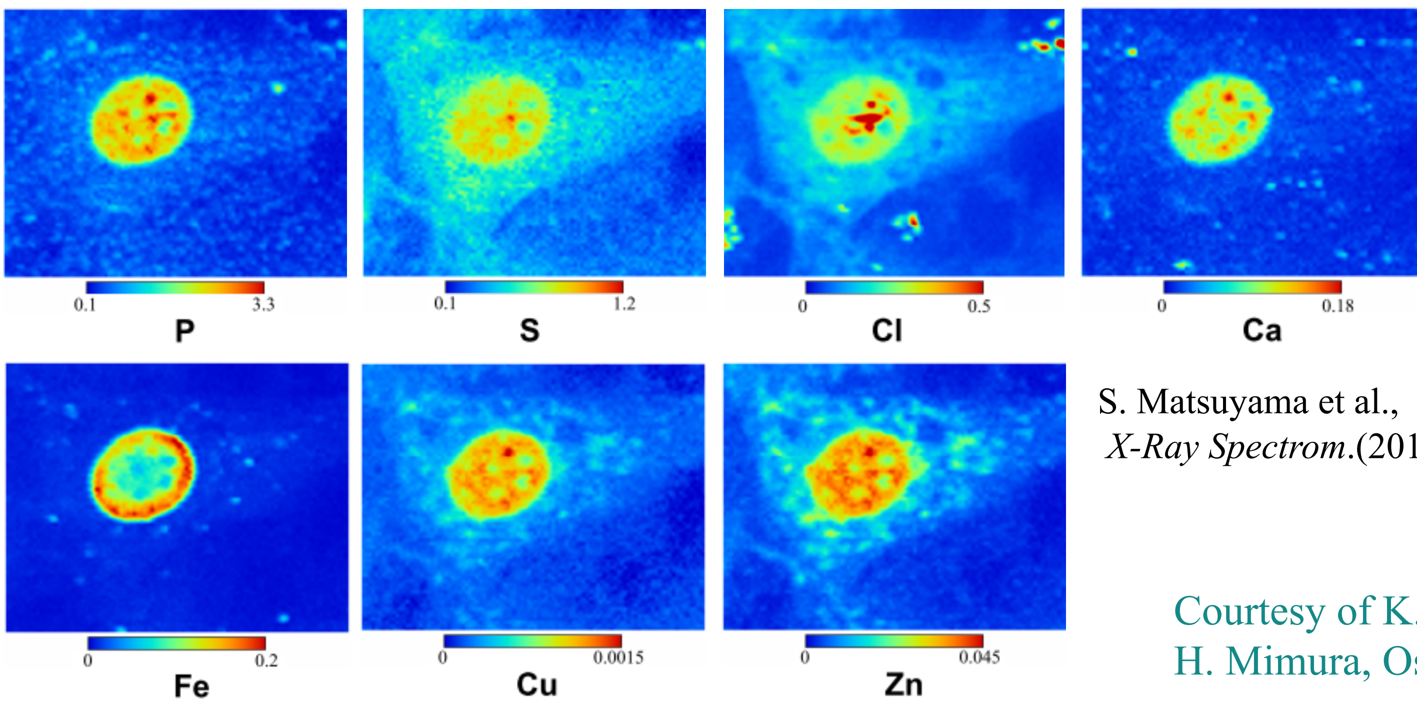

S. Matsuyama et al., *X-Ray Spectrom.*(2010).

Courtesy of K. Yamauchi and H. Mimura, Osaka University.

Breaking the 10 nm barrier in hard x-ray focusing

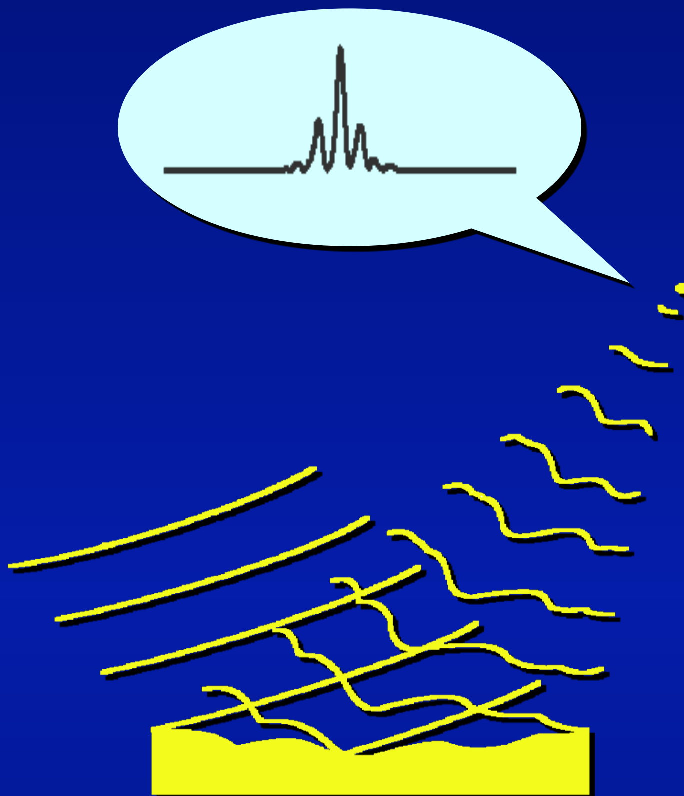

Focusing mirror with phase error

In-situ phase compensation

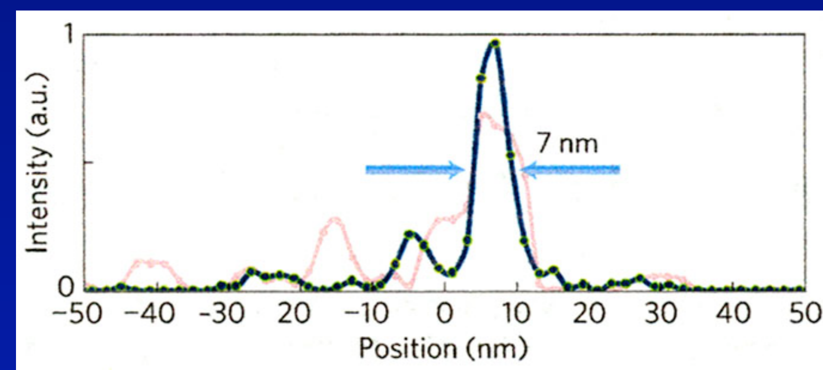

Piezo-electric phase compensator

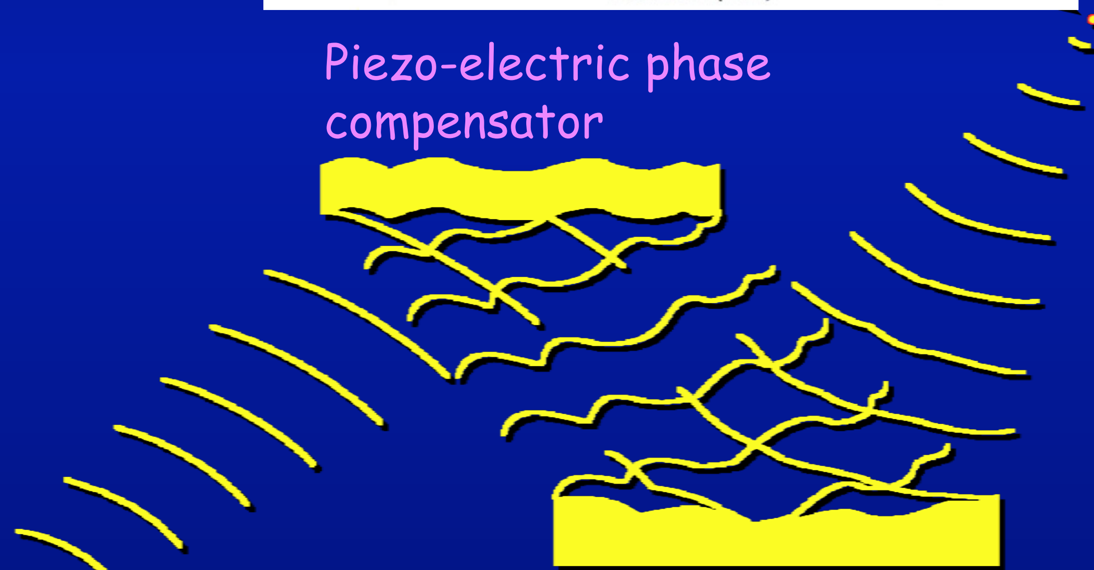

Focusing mirror with phase error

H. Mimura et al., *Nature Physics*, **6**, 122 (2009)

Optical configuration for active phase compensation

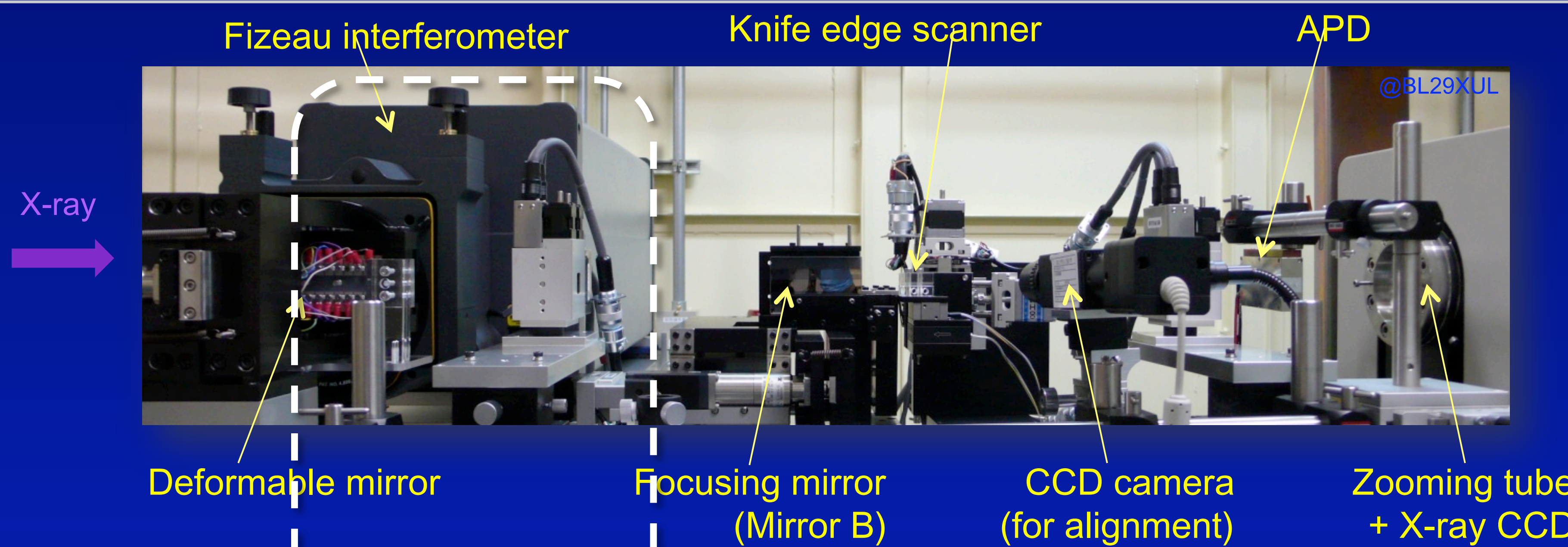

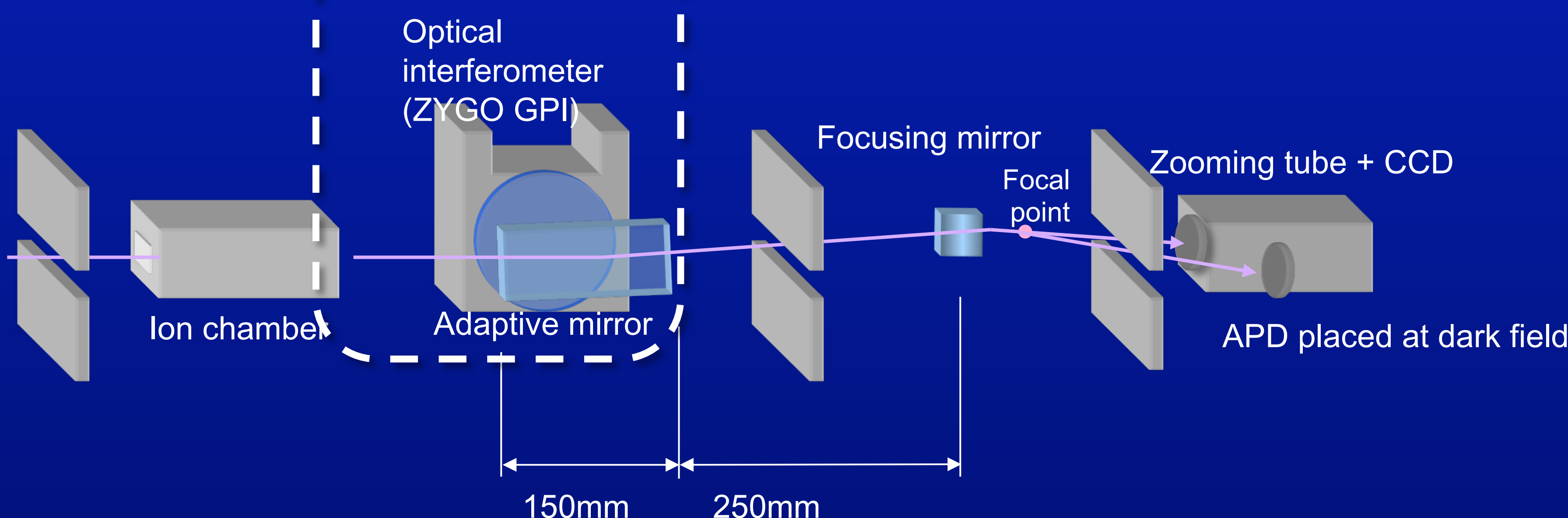

H. Mimura et al., *Nature Physics*, **6**, 122 (2009)

Synchrotron-based art conservation at ESRF

μ-XRF, μ-XRD, μ-XANES

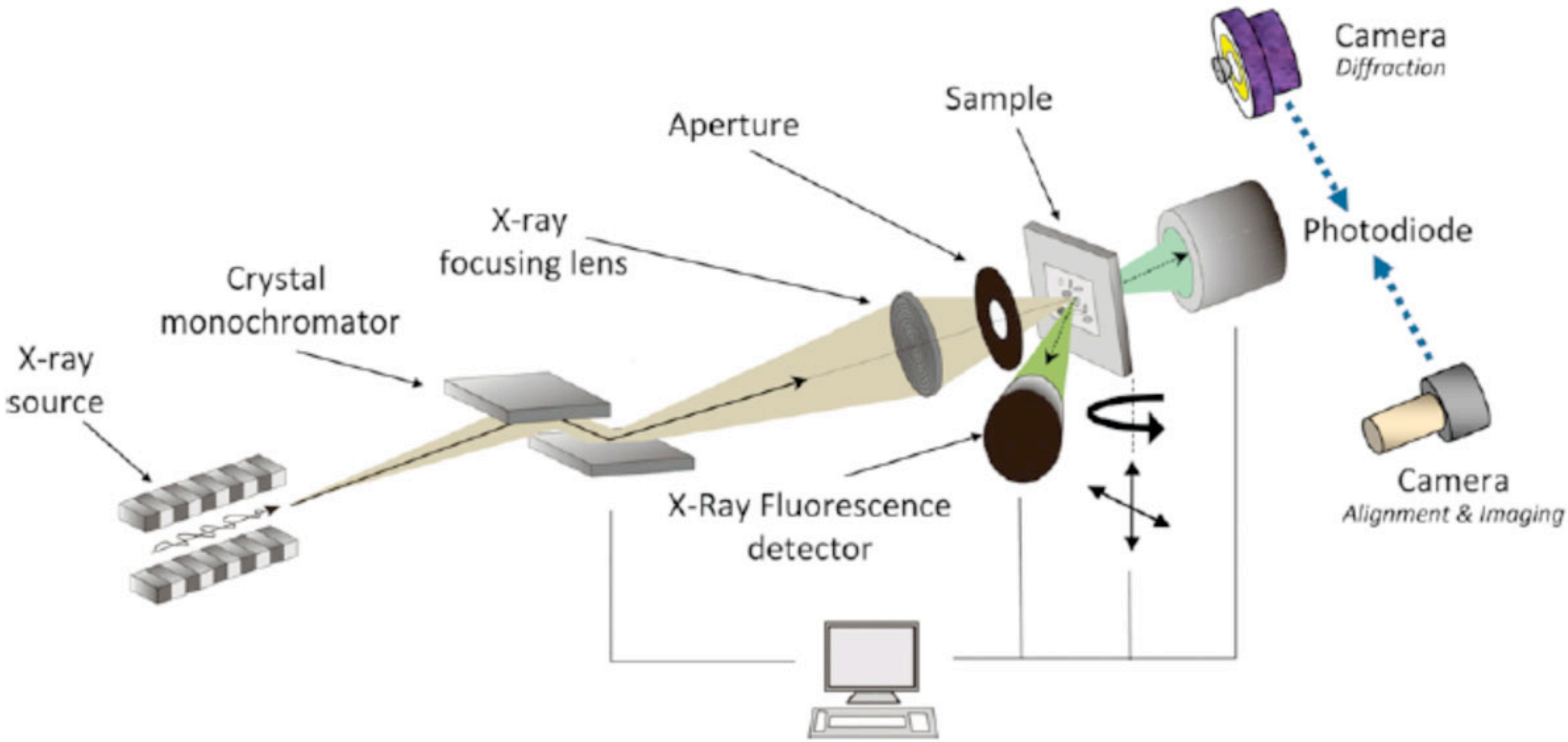

Courtesy of Marine Cotte (ESRF, Grenoble, France)

Examples of µ-XANES K-edge spectra occurring in art materials

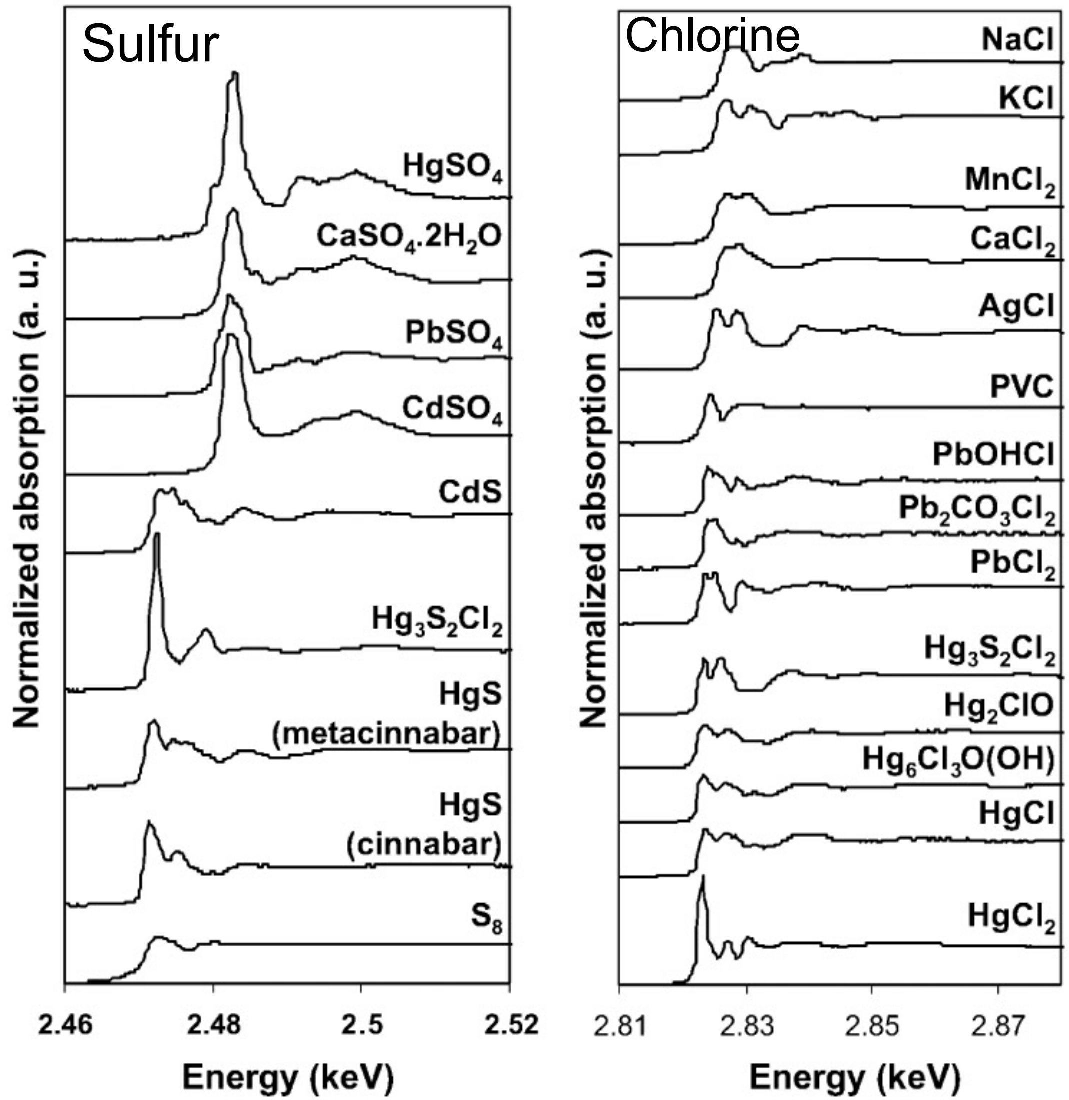

Courtesy of Marine Cotte (ESRF, Grenoble, France)

18^{th} Dynasty Egyptian glass vase studied for an understanding of color and opaqueness in antiquity

1^{st} production of glass objects Egypt (1500 B.C.), opaque, colored, nanoscale calcium antimonate

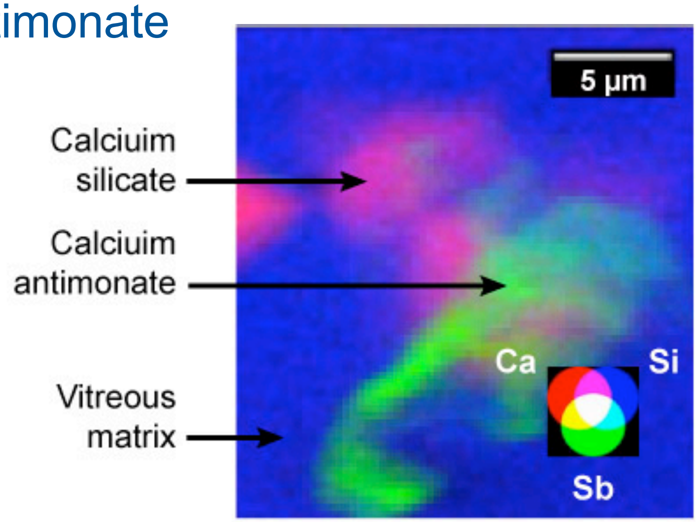

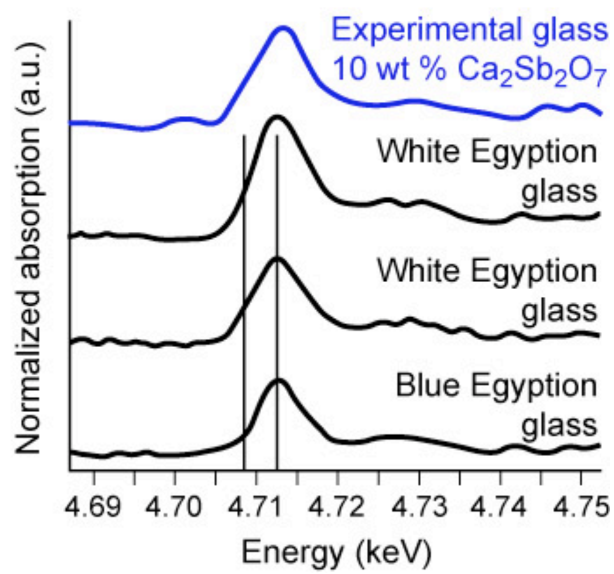

Courtesy of Marine Cotte (ESRF, Grenoble, France)

Synchrotron radiation x-ray tomographic microscopy (SRXTM)

Swiss Light Source

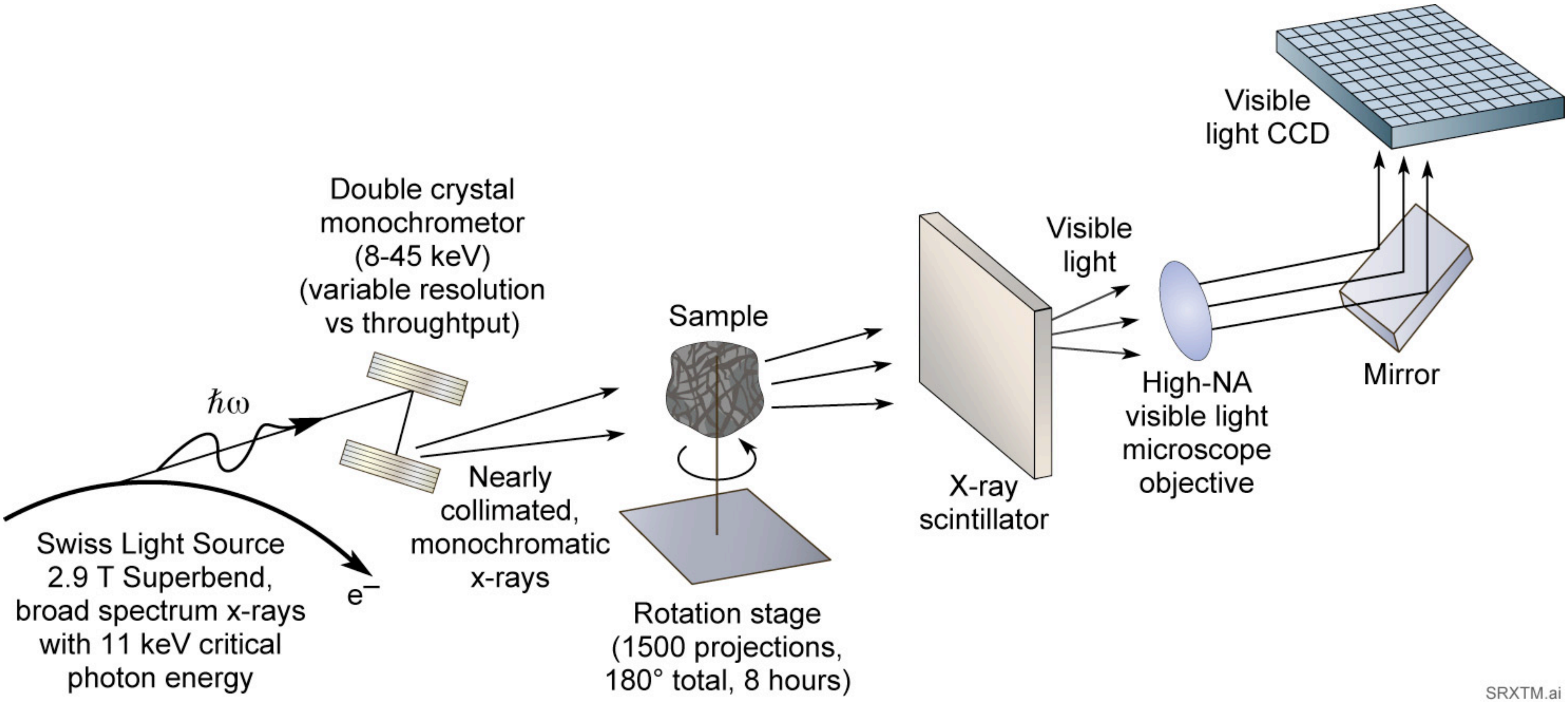

PAUL SCHERRER INSTITUT

Courtesy of Marco Stampanoni, Swiss Light Source.

TOMCAT Microscope

Swiss Light Source

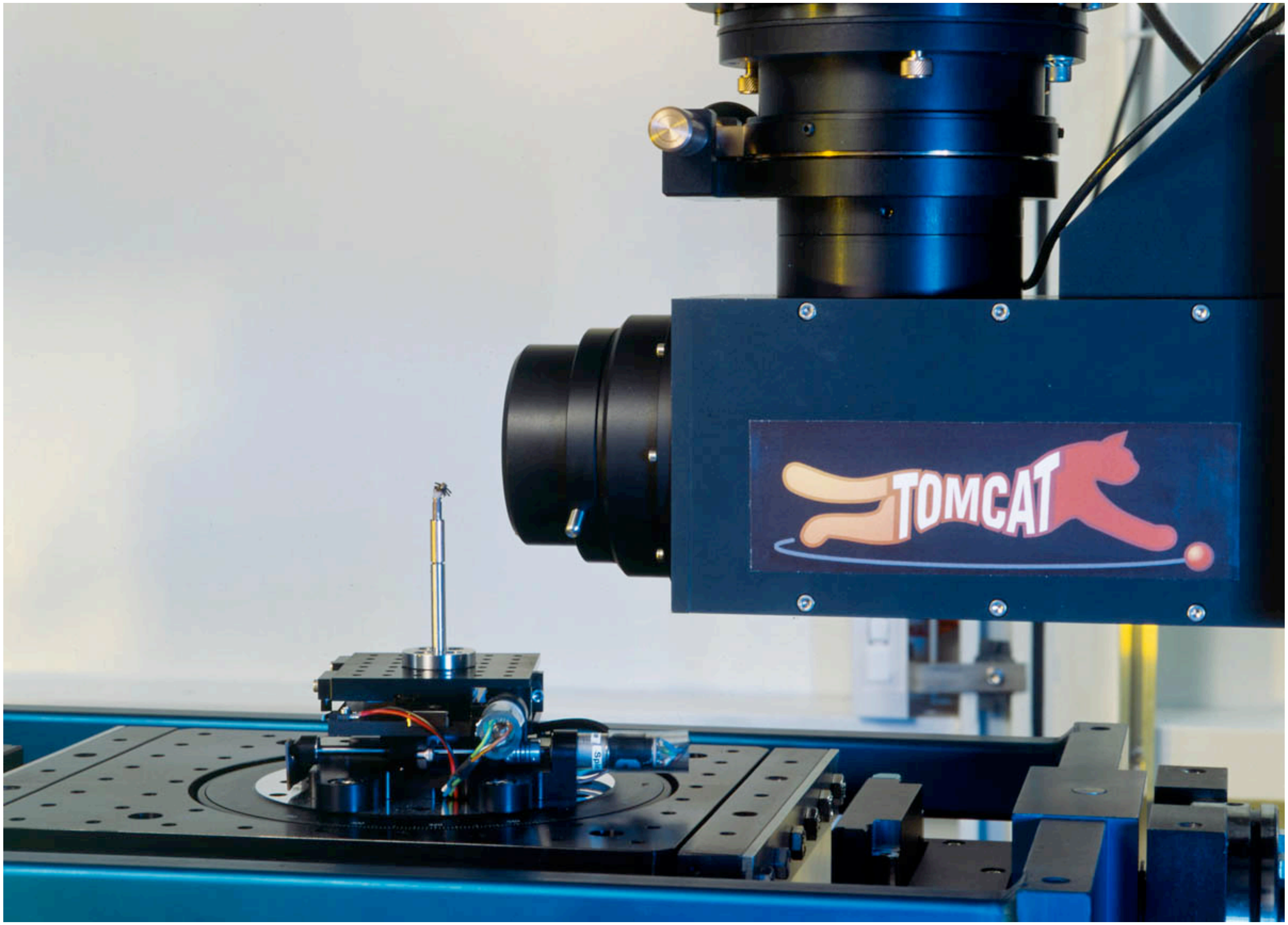

PAUL SCHERRER INSTITUT

1 micron @ 10% MTF reached routinely

Courtesy of Marco Stampanoni, Swiss Light Source.

TOMCAT Microscope

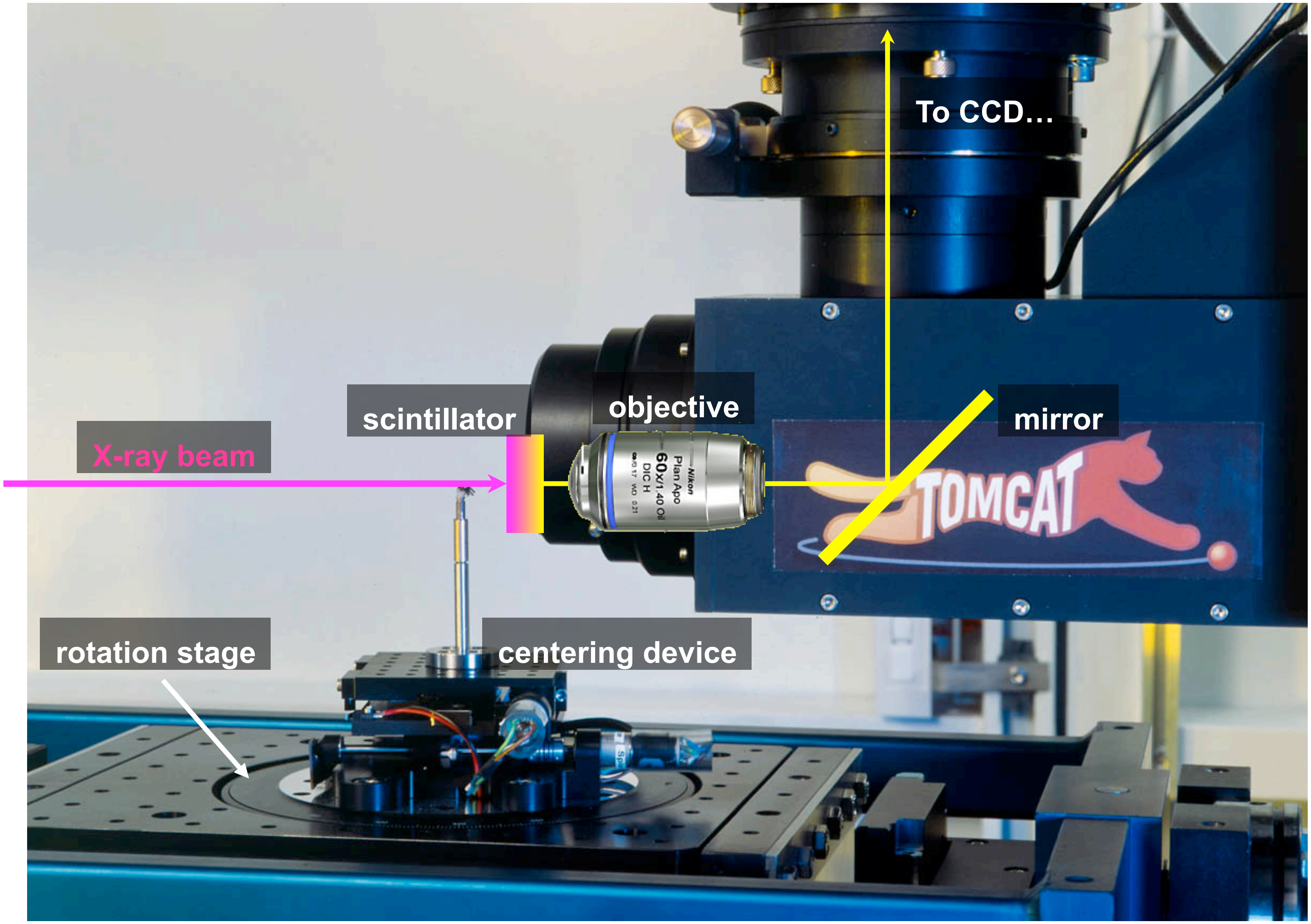

1 micron @ 10% MTF reached routinely

Hard x-ray 3D x-ray tomography: microvascular architecture of a mouse brain

Swiss Light Source

SRXTM, 25 keV,
15 µm resolution
Tomcat Beamline,
Swiss Light Source

M. Stampanoni,
T. Krucker et al.,
Adv. Neur. Res. (2008)

PAUL SCHERRER INSTITUT

Tomographic reconstruction of a 500 million year old fossilized embryo from Southern China

Markelia hunanensis
relative of modern roundworms and arthropods

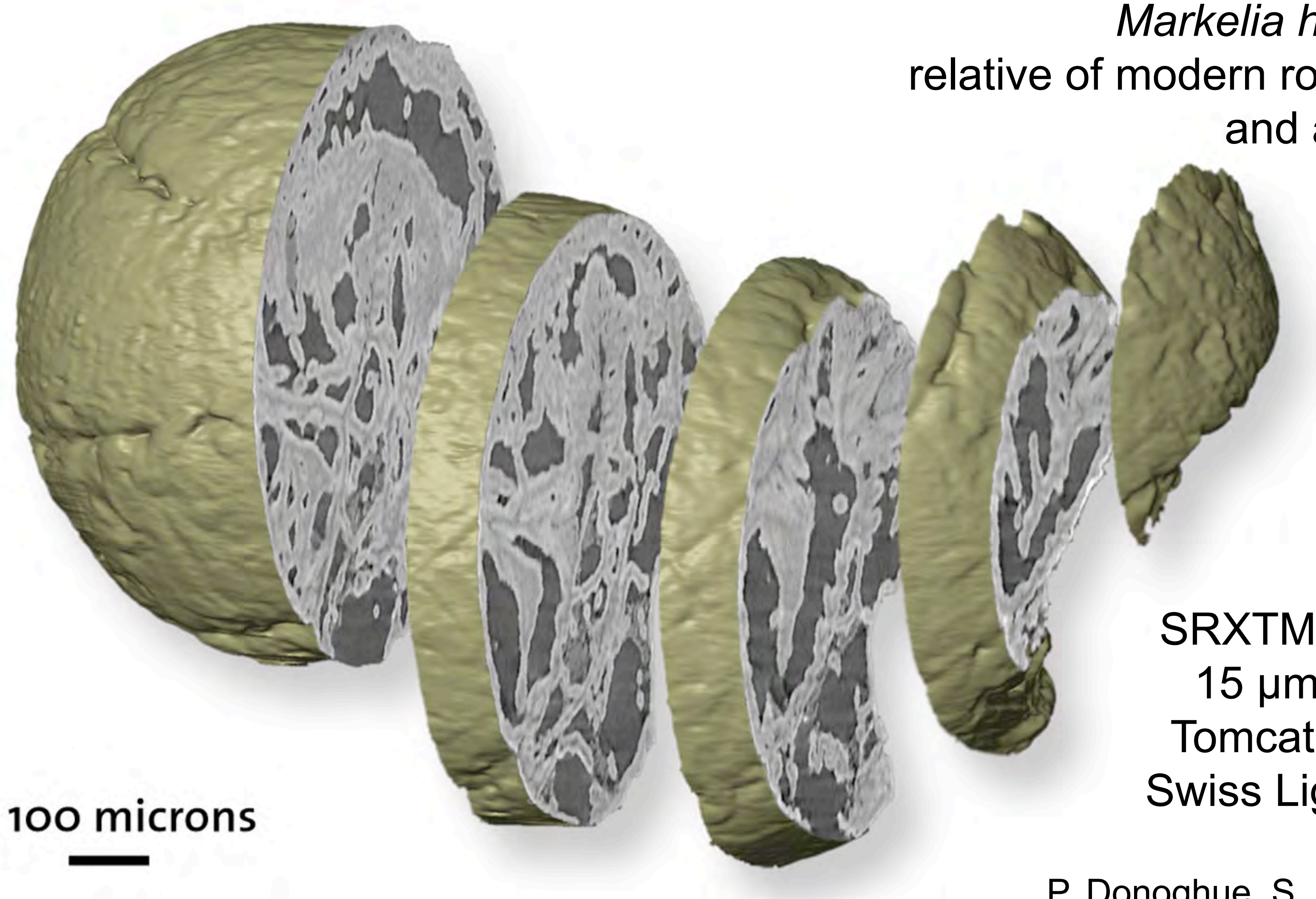

SRXTM, 17.5 keV,
15 µm resolution
Tomcat Beamline,
Swiss Light Source

P. Donoghue, S. Bengtson, M. Stampanoni et al., *Nature* 442, (2006)

A lens is not necessarily required

$\Delta r_{resol.} = k_1 \lambda / NA$

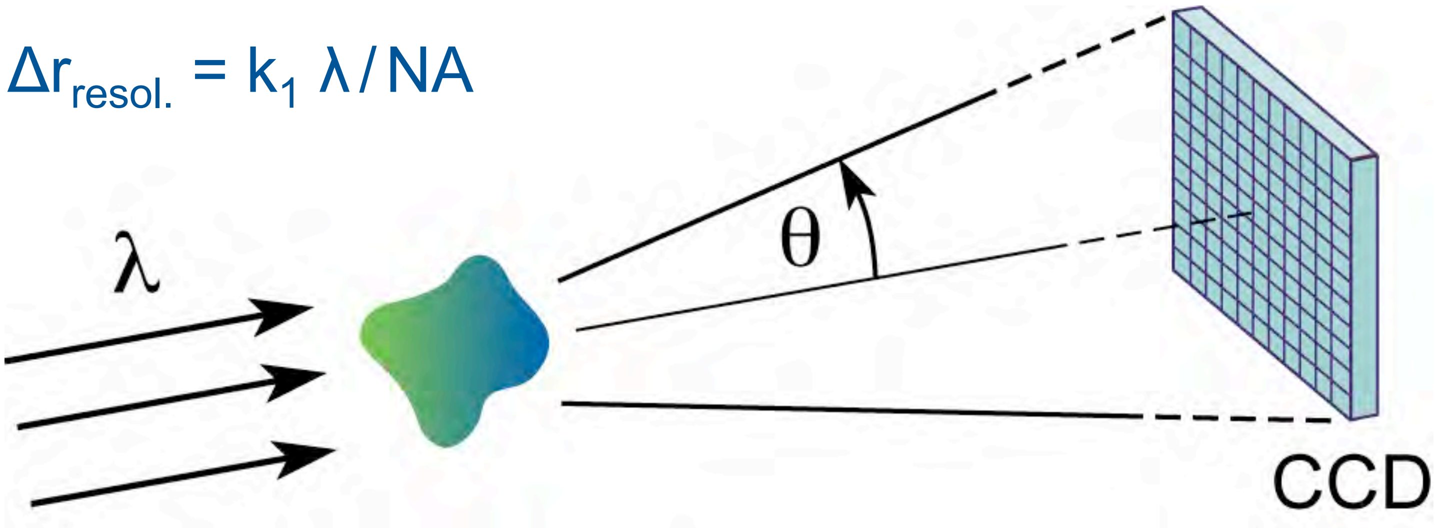

"Lensless" coherent diffraction imaging (CDI) is being aggressively pursued.

Coherent diffractive imaging (CDI)

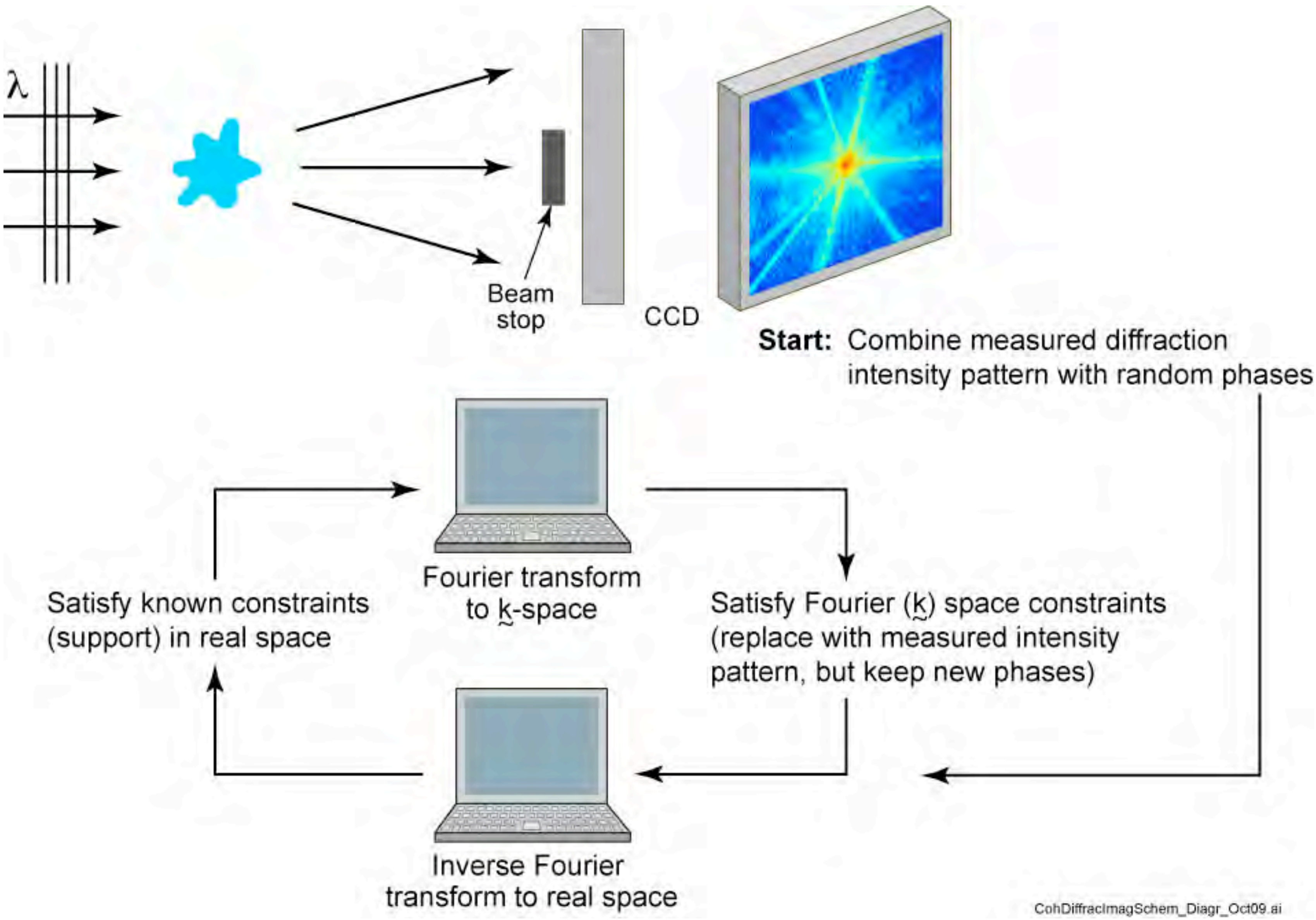

Coherent diffractive imaging (CDI) examples

Femtosecond diffractive imaging with a free electron laser

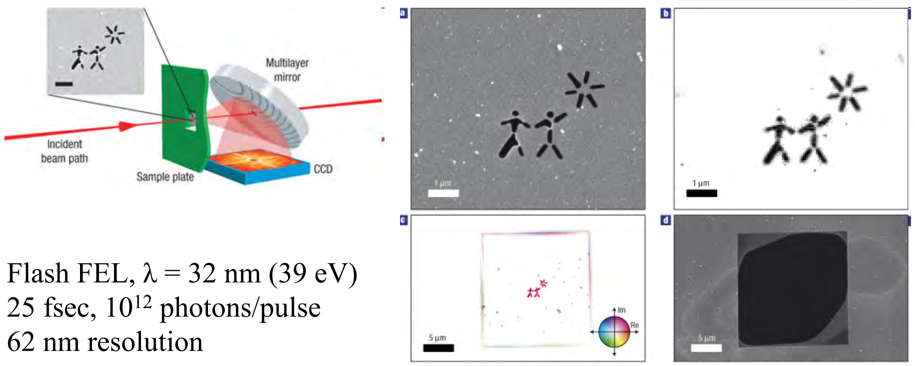

Flash FEL, $\lambda = 32$ nm (39 eV)
25 fsec, 10^{12} photons/pulse
62 nm resolution

Chapman, et al. Nature Physics (2006)

CDI with laboratory scale high harmonic generation (HHG)

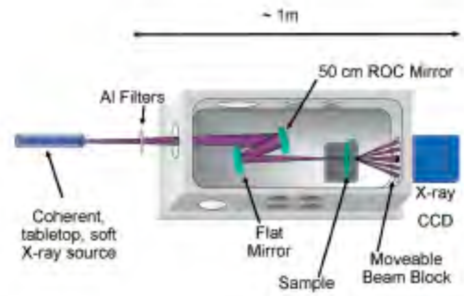

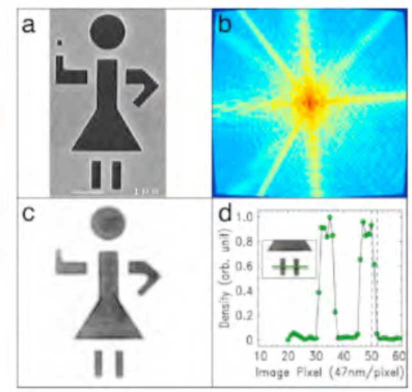

HHG, n = 27, λ= 29 nm (43 eV)
94 nm spatial resolution

Sandberg, et al. PNAS (2008)

Synchrotron based CDI of 100 nm Au spheres

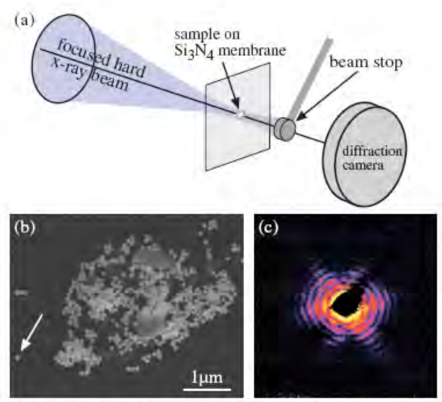

FIG. 1 (color online). (a) Schematic sketch of the coherent diffraction imaging setup with nanofocused illumination. (b) Scanning electron micrograph of gold particles (diameter ≈100 nm) deposited on a Si_3N_4 membrane. (c) Diffraction pattern (logarithmic scale) recorded of the single gold particle pointed to by the arrow in (b) and illuminated by a hard x-ray beam with lateral dimensions of about 100×100 nm^2. The maximal momentum transfer, both in horizontal and vertical direction, is $q = 1.65$ nm^{-1}.

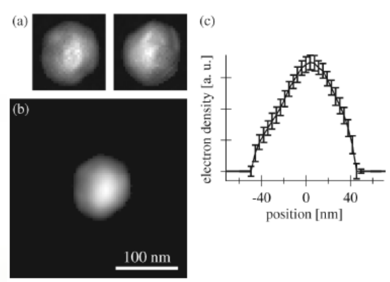

FIG. 2. (a) Two individual reconstructions of the gold particle using the HIO algorithm, a left- and a right-handed one. To obtain the average particle shape from a series of reconstructions with random initial phases, the right-handed reconstructions were inverted and averaged together with the left-handed ones. (b) Reconstructed projected electron density of the gold nanoparticle shown in Fig. 1(b) after averaging the series of reconstructions. (c) Horizontal section through the center of the particle shown in (b). The error bars indicate rms variations in the density for the series of independent reconstructions.

Synchrotron CDI of Au particles
$\lambda = 0.083$ nm (15 keV),
5 nm "resolution"
Schroer, et al. PRL (2008)

Synchrotron based CDI of a freeze dried yeast cell

CDI
ALS/9.0.1
$\lambda = 1.66$ nm
(750 eV)

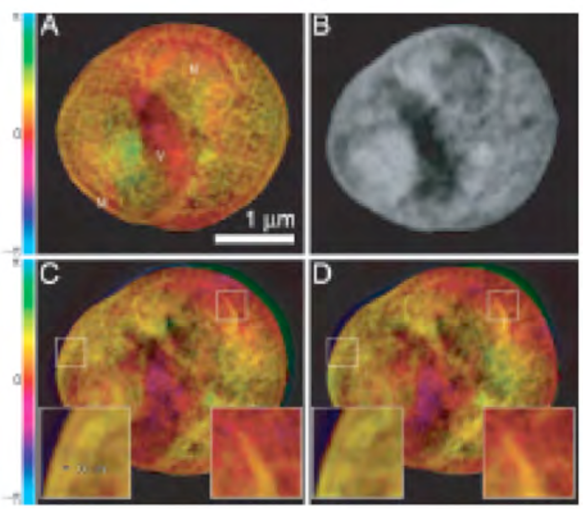

STXM
NSLS/X1
$\lambda = 2.3$ nm
(540 eV)
42 nm
resolution

Tilted 3°

Tilted 4°

30 nm fine features

Shapiro, et al. PRL (2005)

Lensless imaging of magnetic nanostructures by x-ray spectro-holography

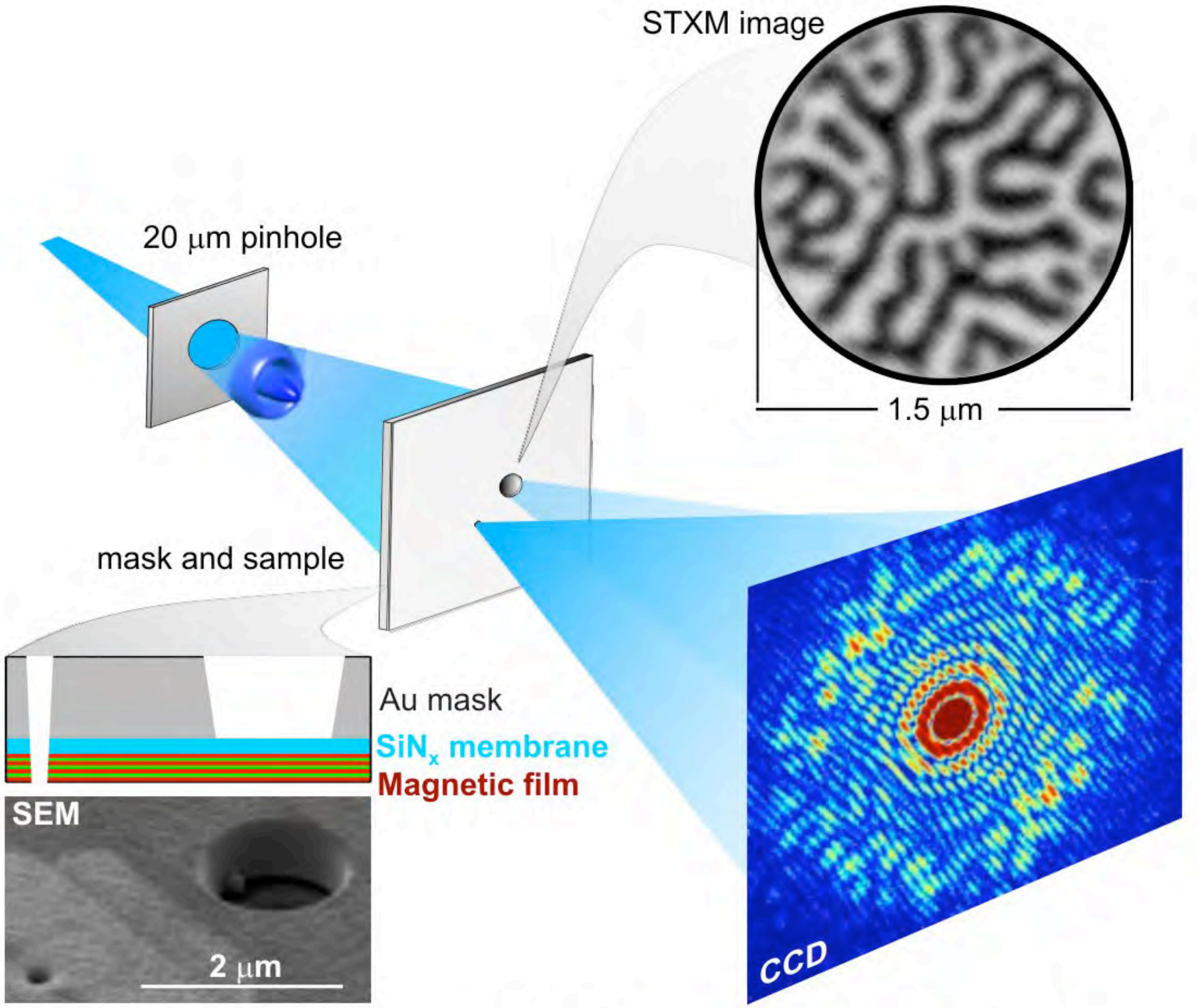

S. Eisebitt, J. Lüning, W.F. Schlotter, M. Lörgen, O. Hellwig, W. Eberhardt & J. Stöhr / *Nature*, 16 Dec 2004

LenslessImagingF1.ai

Lectures online at www.youtube.com

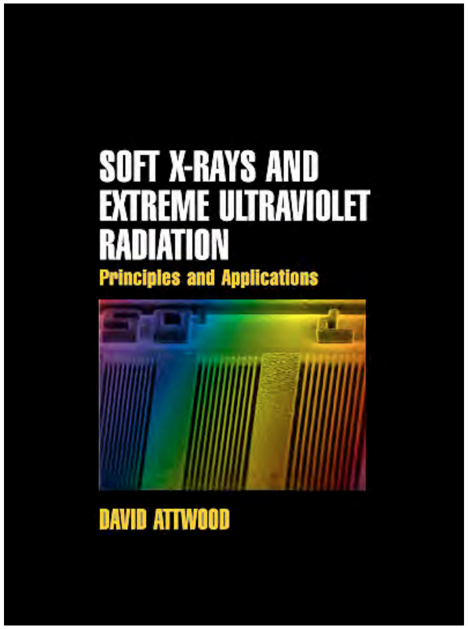

Amazon.com

UC Berkeley

www.coe.berkeley.edu/AST/sxreuv

www.coe.berkeley.edu/AST/srms

www.coe.berkeley.edu/AST/sxr2009